Pergamon

J. Mech. Phys. Solids, Vol. 44, No. 8, pp. 1371–1408, 1996

0022–5096/96 $15.00 + 0.00

PII S0022–5096(96)00020–8

ERICKSEN'S BAR REVISITED: ENERGY WIGGLES

LEV TRUSKINOVSKY† and GIOVANNI ZANZOTTO‡

†Department of Aerospace Engineering and Mechanics, University of Minnesota, Minneapolis, U.S.A.; and ‡Dipartimento di Metodi e Modelli Matematici per le Scienze Applicate Università di Padova, Padova, Italy

(*Received* 24 *October* 1995)

ABSTRACT

This paper addresses the non-uniqueness pointed out by Ericksen in his classical analysis of the equilibrium of a one-dimensional elastic bar with non-convex energy. According to Ericksen, for the bar in a hard device, the piecewise constant functions delivering the global minimum of the energy can have an arbitrary number N of discontinuities in strain (phase-boundaries). Following some previous work in this area, we regularize the problem in order to resolve this degeneracy. We add two non-local terms to the energy density: one depends on the high (second) derivatives of the displacement, the other contains low (zero) derivatives. The low-derivative term (scaled with a constant β) introduces a strong non-locality, and simulates a three-dimensional interaction with the loading device, forcing the formation of layered microstructures in the process of energy minimization. The high-derivative (strain-gradient) term (scaled with a different constant α), represents a surface energy contribution which penalizes the formation of phase interfaces and prevents the infinite refinement of microstructures. In our description we consider the positions of interfaces as variables. This singles out in a natural way an infinite number of finite-dimensional subspaces, where all the essential nonlinearity is concentrated. In this way we can calculate explicitly the local minimizers (metastable states) and their energy, which turns out to be a multi-valued function of the interface positions and the imposed overall strain d. Our approach thus gives an explicit framework for the study of the rich variety of finite-scale equilibrium microstructures for the bar and their stability properties. This allows for the study of a number of properties of phase transitions in solids; in particular their hysteretic behavior. Among our goals is the investigation of the phase diagram of the system, described by the function $N(d, \alpha, \beta)$ giving the number of phase-boundaries in the absolute minimizer. We observe the somewhat counterintuitive effect that the energy at the global minimum, as a function of the overall strain, generically develops non-smooth oscillations (wiggles). Copyright © 1996 Elsevier Science Ltd

Keywords: A. phase transformation, A. twinning, B. crystal plasticity, C. variational calculus, hysteresis.

1. INTRODUCTION

Experimental observations of stress- and deformation-induced phase transitions and twinning in solids reveal fine layered microstructures in a great variety of configurations, and in the last two decades there has been a considerable effort to describe these and related phenomena in terms of elasticity theory. In general, this approach is based on the absolute minimization of a non-(quasi) convex elastic energy for the material, representing a far-reaching generalization of the van der Waals fluid. The relevance of these ideas in the elastostatics of crystalline solids has become clear since Ericksen's analysis (1975) of the highly non-unique minimizers for an elastic bar with a non-monotone stress–strain relation.

The formation of microstructures (phase and twin mixtures) in "non-elliptic"

elasticity reflects the fact that the energy functional is not lower semi-continuous, and thus lacks minimizers. The refinement of phase mixtures can be interpreted as a manifestation of the material striving, by means of minimizing sequences of deformations which develop rapid oscillations, to reach the infimum of its elastic energy while meeting the imposed boundary conditions. Typical examples of observed phase arrangements include rather regular patterns due to piecewise homogeneous layering of twins in fine bands (see Fig. 1). Some basic features of the microstructures (including their phase fraction and orientation) are captured by the existing theory [see James (1992) for a recent review]. However, the absolute minimization of the elastic energy cannot predict some important features like the finite scale of the phase-layering because it forces, instead, an infinite refinement of the microstructure.

While there are also dynamic reasons for the occurrence of finite-scale microstructures [see for instance Ball *et al.*, (1991); Friesecke and McLeod (1994)], a classical way to regularize the problem and obtain finite-scale oscillations in the equilibria is to introduce a strain-gradient contribution ("surface energy") in the potential, which penalizes the formation of regions with rapid changes in strain.

Elastic plus surface energy minimization has been considered by various authors, especially in connection with layered patterns involving two phases. Although the microstructures have mostly been dealt with as essentially one-dimensional in character [see for instance Khachaturyan (1983)], recent results by Kohn and Müller (1992) show that near the boundaries, energy minimization by fine layering is at least a two-dimensional phenomenon. One consequence of this is that the energy scaling is different from that usually assumed. While the above considerations seem to weaken the relevance of one-dimensional models, the observed patterns are, at least locally and away from boundaries, grossly one-dimensional in character, and we adopt here this simplifying assumption.

Indeed, we consider a one-dimensional bar containing a "mixture" of two homogeneous elastic components. For instance, one component may describe the austenitic phase of a multiphase elastic material, while the other corresponds to a homogenized fine layering of different variants of the martensitic phase of the same substance. The bar interacts with an elastic substratum which mimics the three-dimensional boundary conditions constraining surface displacements. This induces microstructural refinement, whereas the "surface tension" contribution to the energy drives the system to minimizing the number of interfaces. A similar approach has already been considered in the literature [see Müller (1990, 1993)].

In this paper we give a framework for the detailed investigation of the variety of stable and metastable equilibria that become available to the system, for a wide range of imposed boundary conditions. Our aim is to clarify the role of interfacial energy in creating finite-scale microstructures, by considering the combined effect of the oscillation-inducing and oscillation-inhibiting terms in the energy functional.

We develop our main considerations under fairly general constitutive assumptions, and we find that the elastic and phase-equilibria for the bar are obtained by piecing together smooth solutions of ODEs, according to appropriate jump and boundary conditions. This allows for the study of the energy landscape in an infinite dimensional space, which can be made explicit at least in the case of quadratic energy density for each phase.

Fig. 1. Multiply twinned nanometer size plate of Ni_4Al_3 growing in B2 austenite. From Schryvers *et al.* (1994).

The expectation that our elementary model will in fact give interesting insight about finite-scale microstructures is supported by the analysis of Müller (1993). For a special case of our boundary conditions, and under the assumption of a smooth two-well energy, he determined the asymptotic behavior for the number of interfaces in the absolute minimizer, in the limit of vanishing surface tension and finite stiffness of the substratum. What is most remarkable, he also could prove the periodicity of the minimizers, which of course is not the case for the general boundary conditions we consider.

Our analysis complements Müller's in that we focus on the local minimizers of the energy. This allows us to address a number of interesting questions that are still quite unclear regarding the general theory of phase transitions in solids, and about which the existence of finite-scale metastable microstructures is likely to have great relevance. One issue is the markedly hysteretic behavior which is typical for solids undergoing phase transformation. As is well known, the study of absolute minimizers cannot account for the hysteresis in the load–deformation curves observed experimentally (Müller *et al.*, 1991; Fu *et al.*, 1992; Ortín, 1992), while the material getting locked in metastable states is a likely cause of such phenomena. A clear suggestion about this comes for instance from the calculations regarding a discrete system of bistable elements (snap-springs) by Müller and Villaggio (1979) and Fedelich and Zanzotto (1992). The investigation of the hysteretic behavior in solid-to-solid transformations is also the subject of recent work by Abeyaratne *et al.* (1994), Ball *et al.* (1994), and Kinderlehrer and Ma (1994). Other questions that our model addresses include the formation of finite nuclei as a mechanism for microstructure refinement, and the assessment of the energy barriers between different equilibrium configurations [cf. also Truskinovsky and Zanzotto (1995)].

In Section 2 we motivate our choice of the energy functional and show how finite spatial oscillations are forced in the equilibria by the competition among the two-well elastic energy of the material, the energy of the elastic foundation (low-derivative contribution and strong non-locality, scaled with a constant β), and the interfacial energy (high-derivative regularization and weak non-locality, scaled with another constant α).

In Section 3 we formulate the model in which a multi-valued strain energy is used to describe the material as a mixture of two phases. We introduce a finite system of transition points where the material switches energy branches : this splits the problem into a infinite-dimensional convex part and finite-dimensional non-convex part. Physically, this corresponds to the uncoupling of the fast, purely elastic modes, from the slower "reconstructional modes" related to the displacement of the interfaces in the reference configuration.

The difference between elastic and phase-equilibria is accordingly discussed in Section 4, where we also perform the step-wise minimization procedure of the energy based on the splitting of the problem. In the same way, we show that the study of stability can be reduced, in our case, to a finite-dimensional problem.

By using the classical methods of variational calculus we derive in Section 5 the conditions of elastic and phase-equilibrium. In Section 6 we discuss the main symmetries of the system and in Section 7 we introduce a constitutively simplified framework, in which the two branches of the elastic energy density are given by two parabolas. This simplification allows us to carry all the computations through with minimal difficulty.

In Section 8 we find explicitly the extremals of the energy for the bar in a hard device with zero, one and two interfaces, and discuss their most significant properties. For simplicity, we limit our examples to equilibria with just a few interfaces, observing even in these cases a great variety of morphologies when the imposed overall strain d and the physical parameters α and β are varied. In Section 9 we discuss some implications of our model and make a few final remarks.

We dedicate this paper to Professor J. L. Ericksen on his seventieth birthday.

2. MOTIVATION

In his paper "Equilibrium of bars" (1975), Ericksen considered a classical problem of equilibrium for a bar in a hard device, which reduces to the minimization of the energy functional

$$E = \int_0^1 f(u')dx, \tag{2.1}$$

with boundary conditions

$$u(0) = 0, \quad u(1) = d, \tag{2.2}$$

where u is the displacement and d the overall imposed strain. If $f(u')$ is convex, the problem is known to have a unique classical solution which, however, cannot account for phenomena such as phase transitions in solids. In order to discuss material instabilities, Ericksen assumed, following earlier ideas by van der Waals about fluids, that the energy density be non-convex [see Fig. 2(a)]; without loss of generality one can consider

$$f(u') = \tfrac{1}{4}[(u')^2 - 1]^2. \tag{2.3}$$

He showed that for d in $[-1, 1]$ the solutions of the minimization problem based on (2.1–2.3) exhibit a dramatic lack of uniqueness. In fact, any continuous displacement u giving a measurable mixture of the two states $u' = \pm 1$ (with the portion of the bar in each state prescribed by d), is a solution. What is left unspecified are details of the partition of the bar into phases, among which is N, the number of interfaces. These details depend on various physical aspects of the phenomenon, which are missing in the model (2.1–2.3).

Some mechanisms that can narrow the non-uniqueness and bring a desired selection principle were identified long ago. For instance, the problem can be regularized by introducing a penalization for the formation of (sharp) interfaces. This method again dates back to van der Waals and leads to considering a dependence of the energy density on the higher derivatives. The simplest functional with which to substitute (2.1) is

$$E = \int_0^1 [f(u') + \alpha(u'')^2]dx, \tag{2.4}$$

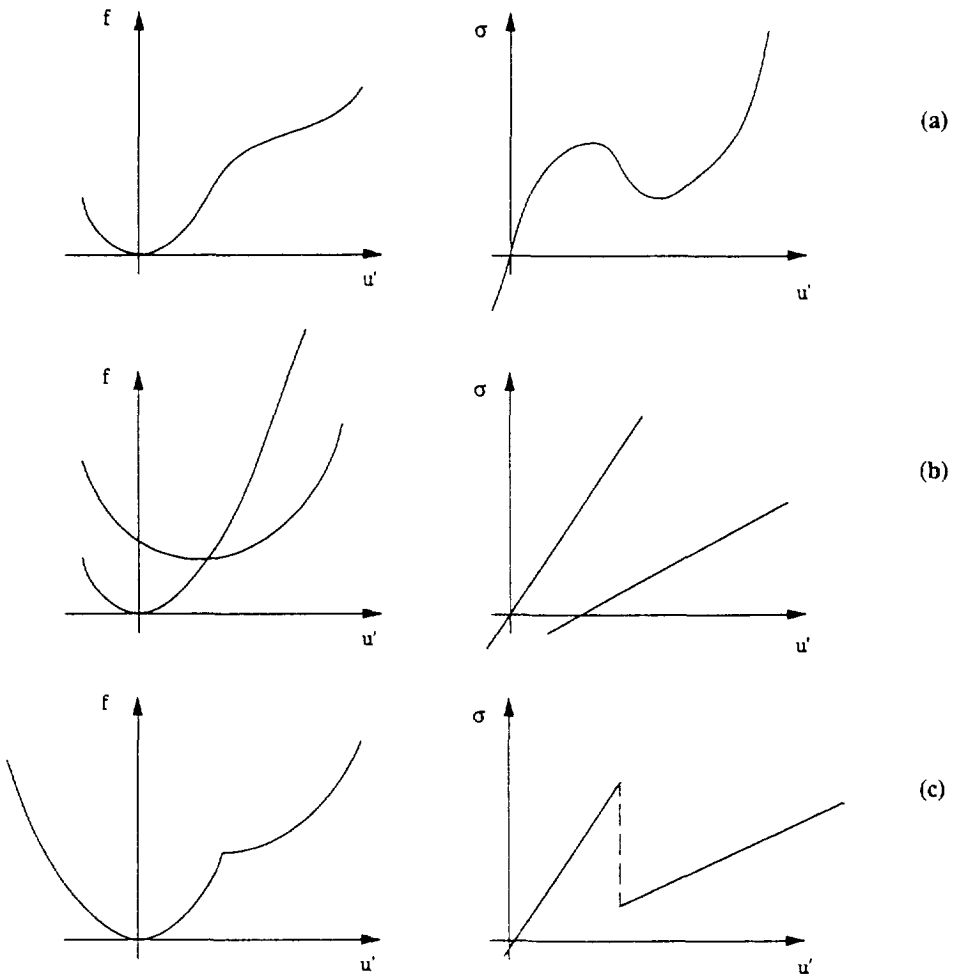

Fig. 2. Three possible energy density functions and the corresponding stress–strain relations. (a) A smooth non-convex energy. (b) The smooth and convex energies of the two components of a mixture, each defined for all strains. (c) The same energy as in (b) in which the multi-valuedness is eliminated : it can be considered as a non-smooth approximation for the energy in (a).

where α is a positive coefficient giving rise to an internal length-scale in the system. The analysis of the minimization problem based on (2.4) and (2.2) and (2.3) shows that the absolute minimizer is now unique, but the number N of interfaces is exactly equal to one (Carr *et al.*, 1985). This does not always reflect the experimental observations (see Fig. 1) : the reason is that the mechanism favoring multiple interfaces is still missing in this approach [see, however, Parry (1989)].

An alternative to the model based on (2.1) and (2.3) comes from the observation that periodic microstructures arise in situations that are at least two-dimensional. Indeed, in two- or three-dimensional models the interaction with the environment causes the development of oscillations in the solutions because the displacements are

much more severely constrained by the boundary conditions than in one-dimensional problems. In order to obtain an analogous effect, one can place the one-dimensional bar on an elastic foundation. Then (2.1) and (2.3) are substituted by

$$E = \int_0^1 [f(u') + \beta u^2] dx, \tag{2.5}$$

where the positive constant β models the stiffness of the "elastic matrix". The solution of the minimization problem based on (2.5) and (2.2) for $d = 0$ is known from the times of Bolza [see for instance Young (1980)]. In this case, the absolute minimizer does not exist, and the minimizing sequences exhibit finer and finer mixtures of the two phases with $u' = \pm 1$. One can say that in this model the number N of interfaces becomes infinite, which is again not satisfactory if the goal is the description of a realistic microstructure as the one shown in Fig. 1.

It is thus quite natural to consider a combination of the two previous models; that is, to replace (2.1) with the functional

$$E = \int_0^1 [f(u') + \alpha(u'')^2 + \beta u^2] dx, \tag{2.6}$$

and view Ericksen's bar as a limit for $\alpha \to 0$ and $\beta \to 0$. Owing to the interaction between the two terms depending on α and β in (2.6), one can expect to obtain equilibrium configurations with different $N = N(d, \alpha, \beta)$. Müller (1990, 1993) considered the special case $\beta = 1$ and $d = 0$. One of the goals of this paper is to obtain some information about the phase diagram of the system in (d, α, β)-space, by finding the stability domains for equilibria with different N.

The fact that this diagram is non-trivial can be illustrated by the following elementary analysis. Consider the special case $d = 0$, and observe that the Euler–Lagrange equation

$$2\alpha u'''' - [f''(u')]' + 2\beta u = 0 \tag{2.7}$$

for the minimization problem (2.6) with (2.2) and (2.3), has a trivial solution $u \equiv 0$. In order to study the linear stability of this solution, introduce a perturbation as

$$u^*(x) = \sum_{p=1}^{4} A_p \exp(k_p x). \tag{2.8}$$

It is standard to show that a non-trivial solution of the linearized version of (2.7) exists if

$$k_{1,2,3,4} = \pm \left(\frac{-f''(0) \pm (f''(0)^2 - 16\alpha\beta)^{1/2}}{2\alpha} \right)^{1/2} \tag{2.9}$$

and

$$\alpha\pi^4 n^4 + \beta = -\tfrac{1}{2} f''(0) \pi^2 n^2. \tag{2.10}$$

This means that there exists an infinite number of instability modes of the trivial

solution parametrized by an integer n. Equation (2.10) gives the stability boundary of this solution in (α, β)-space (at $d = 0$). The result is a piecewise linear curve whose corners indicate transitions between regimes with a different number of oscillations: it suggests that for sufficiently small α and β, there exist separate stability regions for equilibria with different numbers of "interfaces". The occurrence of stability diagrams of piecewise smooth nature is not surprising; in fact the linearized version of (2.7) with $f''(0) = -1$ reproduces the classical equation for a beam on an elastic foundation, if the longitudinal force $p \sim \alpha^{-1}$ and the thickness $h \sim \beta\alpha^{-1}$ are considered as parameters. The piecewise smooth (p, h)-bifurcation diagrams for the beam are well known in the engineering literature. An analogous effect is observed also in the theory of shells [see, for instance, Graff *et al.* (1985)].

A simple argument, similar to the one used by Khachaturyan (1983) in a different context, gives us the asymptotics for $N(d, \alpha, \beta)$ originating from (2.6) for small α and β such that $\beta \gg \alpha^{1/2}$ (which means large N) and $d = 0$. Consider a mixture of two states that minimizes the energy (2.6) in the limit for $\alpha \to 0$ and $\beta \to 0$ and $d = 0$. One expects that $u' = 1$ or $u' = -1$ everywhere except for the narrow transition layers (modeling the "interfaces") whose thickness is proportional to $\alpha^{1/2}$. Inside the thin interface layer the role of the elastic foundation is negligible so the following Euler–Lagrange equation holds: $\alpha(u'')^2 = f(u')$, and the corresponding contribution to the energy is [see, for example, Müller (1993)]

$$\int_{\text{interfaces}} [f(u') + \alpha(u'')^2]dx = 2\alpha^{1/2} \int_{-1}^{1} f(w)^{1/2} dw.$$

It follows that the "surface" plus elastic energy concentrated inside each layer is proportional to $\alpha^{1/2}$. By considering solutions with N interfaces (N large), we obtain

$$\int_0^1 [f(u') + \alpha(u'')^2]dx \sim \alpha^{1/2} N. \tag{2.11}$$

In order to estimate the elastic energy accumulated in the substratum, we can suppose that the interfaces are almost equidistant from each other. Then the period of the microstructure is of the order of N^{-1}, and since $u' = \pm 1$, it is not hard to see that, for large N

$$\int_0^1 \beta u^2 dx \sim (\beta/12) N^{-2}. \tag{2.12}$$

Furthermore, in this limit the "elastic" energy of the bar is negligible outside the transition layers. Hence the total energy is reduced to the contribution (2.11), which is proportional to N, plus the term (2.12) that goes to zero as N goes to infinity. The energy minimum is achieved when

$$\alpha^{1/2} N = \text{const}\, \beta N^{-2}, \tag{2.13}$$

or

$$N(0, \alpha, \beta) \sim \beta^{1/3} \alpha^{-1/6}. \tag{2.14}$$

This gives the desired asymptotics. Müller (1993) has given a detailed derivation of this estimate in the special case $\beta = 1$, which also includes a proof of the periodicity of the absolute minimizer (a property true only for $d = 0$). We notice that (2.14) is an example of intermediate asymptotics in the sense of Barenblatt (1995) since the function $N(0, \alpha, \beta)$ has no classical limit for $\alpha \to 0$ and $\beta \to 0$; this is the main reason of the non-uniqueness pointed out by Ericksen. Indeed,

$$N(0, \alpha, \beta) \sim \gamma^{1/3}, \tag{2.15}$$

where

$$\gamma = \beta \alpha^{-1/2}, \tag{2.16}$$

this means that in the limit of small α and β the system behaves differently according to how such a limit is reached, "remembering" the limit of the ratio $\beta\alpha^{-1/2}$.

We conclude from this argument that the boundaries of the stability domains for equilibrium microstructures with different (large) N in the (α, β) phase diagram for $d = 0$ can be described by the simple asymptotic relation

$$\alpha = C\beta^2, \tag{2.17}$$

with C a positive constant.

The above consideration clearly suggest that the model based on the elastic energy (2.6) has a variety of equilibria characterized by a finite number of internal transition layers, which is the feature we sought for. However, from a physical standpoint there still are some limitations in the setting of the problem that should be taken into account, in order that the model be capable of giving an adequate description of the following important aspects of solid-to-solid transitions.

(i) There is experimental evidence that phase-boundaries can be locked while the elastic field relaxes, and that they will not adjust their positions in the reference configuration simultaneously with it, demonstrating, in fact, a considerable delay. Experiments in which partial unloading (under controlled d) is performed on shape-memory alloys can be interpreted as if "elastic equilibria" (with "frozen" interfaces) and "phase-equilibria" (with "relaxing" interfaces) are distinguished (Fu *et al.*, 1992).

(ii) The model with strain energy (2.3) describes a material with displacive transformations and is most relevant for a one-dimensional description of twinning. It assumes that one lattice can be transformed continuously into another and that there is an unstable spinodal region with $f''(u') < 0$. However, in solid-to-solid phase transitions other phenomena are often observed which are not well described by a single-valued energy function such as (2.3). These include the fine mixtures involving interfaces between austenite and twinned martensite, or the solid-state transformations in which not only the lattices are deformed, but also the chemical composition or other parameters like polarization and the degree of order, experience a discontinuity at the interface.

The model should thus be based on a multi-valued energy and should allow for a clear separation of internal variables describing the positions of the interfaces in the reference configuration [see also Parry (1987)]. The simplest one-dimensional generalization of (2.3) along these lines is a model with a double-valued energy

$$f = \begin{cases} f_+(u') \\ f_-(u') \end{cases} \tag{2.18}$$

[see Fig. 2(b)] where the functions $f_+(u')$ and $f_-(u')$ are smooth and convex. Although in this paper we concentrate on the model based on (2.18), we notice that another model with

$$f(u') = \min\{f_+(u'), f_-(u')\} \tag{2.19}$$

can be obtained as an "approximation" of a smooth two-well energy [compare Fig. 2(a) and 2(c)]. We show in Section 5 that in our one-dimensional case the equilibria assuming (2.18) are the same as with (2.19). Moreover, the most important conclusions about the equilibrium microstructures for the model based on the smooth energy (2.3) are still true for (2.18) and (2.19), even though these last do not have a spinodal region. Notice, however, that the stability properties of the equilibria in all these three models are likely to be different. Furthermore, we recall that since (2.19) is a single-valued function while (2.18) is not, there are major differences in the three-dimensional case since, for instance, the three-dimensional analog of (2.18) allows for "elastically equilibriated" ellipsoids (see Eshelby, 1956; Kaganova and Roitburd, 1987), while the three-dimensional analog of (2.19) does not (see Lifshitz, 1948; Rosakis, 1992).

3. THE MODEL

3.1. *Energy*

Denote by $u(x)$ the displacement of the reference point x of a bar $[0, L]$ containing a "mixture" of two homogeneous elastic components, say "+" and "−" (the two "phases" of the material); their energy densities are given by smooth convex functions of the strain u', whose generic plots are represented in Fig. 2(b) [see (2.18)]

$$f = f_+(u') \quad \text{and} \quad f = f_-(u'); \tag{3.1}$$

corresponding stress–strain relations, given by

$$\sigma = \sigma_+(u') = f'_+(u') \quad \text{and} \quad \sigma = \sigma_-(u') = f'_-(u'),$$

are also shown in Fig. 2(b).

We suppose that the total energy functional is given by the sum of three terms

$$E = E_1 + E_2 + E_3. \tag{3.2}$$

The term E_1 gives the amount of elastic energy stored in the bar as the integral of the energy density per unit reference length

$$E_1 = \int_0^L [\chi f_-(u') + (1-\chi) f_+(u')] dx, \tag{3.3}$$

where χ denotes the volume fraction of the "−" phase. We assume that the two

components are separated; therefore, in (3.3) χ is the characteristic function of the subset of $[0, L]$ occupied by the "$-$" component.

The term E_2 is a gradient-dependent contribution

$$E_2 = \alpha \int_0^L (u'')^2 dx, \tag{3.4}$$

with $\alpha > 0$ a constant which provides an internal length-scale proportional to $\alpha^{1/2}$. Finally, we take the form of E_3 in (3.2) to be as follows

$$E_3 = \int_0^L \left\{ \int_0^L G(x, y) u(x) u(y) dx \right\} dy. \tag{3.5}$$

This non-constitutive term describes the energy stored in an elastic substratum due to the deformation of the bar [see Fosdick and Mason (1994) or Brandon and Rogers (1994) for models with a constitutive spatial non-locality]. The simplest assumption regarding the kernel G is $G(x, y) = \beta\delta(x - y)$, with $\beta > 0$ a constant describing the stiffness of the elastic foundation (a continuous system of non-interacting, linearly elastic springs) and δ indicates the Dirac function. The term E_3 thus takes the form

$$E_3 = \beta \int_0^L u^2 dx; \tag{3.6}$$

this introduces a further length-scale, proportional to $\beta^{-1/2}$.

For the purpose of defining non-dimensional variables, let us consider the elastic modulus μ of one of the phases, and set

$$\bar{x} = x/L, \quad \bar{u} = u/L, \quad \bar{f}_\pm = 2f_\pm/\mu, \quad \bar{E} = 2E/L\mu. \tag{3.7}$$

This leaves two essential non-dimensional parameters in our model:

$$\bar{\alpha} = 2\alpha/L^2\mu, \quad \bar{\beta} = 2\beta L^2/\mu. \tag{3.8}$$

The explicit form of the total energy functional (3.2) becomes

$$E[u, \chi] = \int_0^1 [\chi f_-(u_x) + (1 - \chi) f_+(u_x) + \alpha(u_{xx})^2 + \beta u^2] dx, \tag{3.9}$$

where all the superimposed bars on the new variables have been dropped. Notice that although we assume the original parameters α and β to be small, the normalized ones in (3.8) depend on the size L of the bar and are not necessarily small. Thus, for small enough samples, α in (3.9) can be large.

Our present goal is obtaining information about the stable and metastable equilibria of the bar with energy (3.3) in a hard device

$$u(0) = a, \quad u(1) = b. \tag{3.11}$$

This means finding the displacement fields u and the characteristic functions χ such that $[u, \chi]$ constitute (local) minimizers of the functional (3.9) under condition (3.11).

3.2. *Phase mixtures*

We will carry out our study under some simplifying assumptions. First, in order to concentrate our attention only on the physically most relevant solutions, we restrict our attention to arrangements in which the region occupied by each phase is a finite union of intervals. Thus we consider a finite number N of points c_i in $[0, 1]$, $i = 1, \ldots, N$, such that $c_i < c_{i+1} (c_0 \equiv 0, c_{N+1} \equiv 1)$, and require the function χ in (3.9) to be as follows

$$\chi = \chi_{[0,c_1]\cup[c_2,c_3]\cup\ldots} \quad \text{or} \quad \chi = \chi_{[c_1,c_2]\cup[c_3,c_4]\cup\ldots}, \tag{3.12}$$

where $[0, c_1] \cup [c_2, c_3] \cup \ldots$ or $[c_1, c_2] \cup [c_3, c_4] \cup \ldots$ are alternating unions of intervals in $[0, 1]$ whose ends are at the points $c_i, i = 0, 1, \ldots, N+1$. Each such point gives the position of a phase-boundary in the bar, where a switching of components [that is, of energy functions (3.1)] occurs. Notice that because of (3.4), $(3.12)_1$ prescribes that the initial interval $[0, c_1]$ be occupied by the "$-$" phase, while $(3.12)_2$ prescribes $[0, c_1]$ be occupied by the "$+$" phase. In general, these two alternatives are not equivalent; however, we will see that they become symmetry-related under some assumptions regarding the energy functions (3.1) (see Section 6).

Confining our attention to extremals and competitors with a finite number of transition points, we replace the unknown function χ in (3.9) by a finite set of variables $c_1, \ldots, c_N$, whose number N acts as a discrete parameter.

3.3. *The functional*

By (3.9) and (3.12), the energy functional becomes explicitly

$$E = \begin{cases} E_0[u], \\ E_1[u, c_1], \\ \quad \vdots \\ E_N[u, c_1, \ldots, c_N], \\ \quad \vdots \qquad\qquad (N = 0, 1, 2, \ldots) \end{cases} \tag{3.13}$$

whose "branches" are each given by

$$E_N[u, c_1, \ldots, c_N] = E[u, \chi_{c_1,\ldots,c_N}] = \sum_{i=0}^{N} \int_{c_i}^{c_{i+1}} [f_{\pm}(u') + \alpha(u'')^2 + \beta u^2] dx, \tag{3.14}$$

where $\chi_{c_1,\ldots,c_N}$ denotes any of the characteristic functions introduced in (3.12). Each parameter c_i ranges in $[0, 1]$, subject to the condition $c_i < c_{i+1}$. In the integral $(3.14)_2$ it is thus understood that the functions f_- and f_+ are taken alternately in each interval $[c_i, c_{i+1}]$.

In general, (3.13) and (3.14) are defined for any displacement u (necessarily in C^1) whose second distributional derivative is square integrable in $[0, 1]$; however, we make, after (3.12), a second simplifying assumption and confine our attention to a subclass of more regular functions. Indeed, any admissible displacement field u for the functional (3.13) will be required to be at least C^1, piecewise C^2 in $[0, 1]$. This is in

the same spirit as (3.12), which also restricts the allowed arrangements of phases in the bar. We will discuss the competitors in more detail in Section 5.

3.4. *Boundary conditions*

The boundary conditions to be met by all displacements in the hard device are given in general by (3.11). However, in the calculations that follow we will confine ourselves to the discussion of solutions to the symmetric problem

$$u(0) = -d/2, \quad u(1) = d/2. \tag{3.15}$$

In (3.15) the parameter d has the meaning of a non-dimensional measure of the imposed displacements at the ends of the pinned bar. Since we are indeed considering the normalized interval $[0, 1]$, d can also be interpreted as a measure of the average strain in the bar.

Notice that a difference arises between this problem and, for instance the one with boundary conditions

$$u(0) = 0, \quad u(1) = d. \tag{3.16}$$

This originates from the loss of translational invariance in the system due to the non-purely constitutive nature of the contribution (3.5) and (3.6) to the energy. The fact that the boundary conditions (3.15) are symmetric introduces a "geometric" symmetry in the system; this will be discussed in more detail in Section 6. Some results regarding the non-symmetric boundary conditions (3.16) will be briefly presented in Section 7.

4. LOCAL AND ABSOLUTE MINIMIZATION OF THE ENERGY

4.1. *Local minimization; elastic and phase-equilibria*

The particular structure of our energy functional naturally lends itself to a stepwise minimization which breaks down the process into several stages.

Let d and N be given; we must test any candidate local minimizer $[u, c_i]$ $(i = 1, \ldots, N)$ of the energy (3.13) against any admissible competitor in which u, c_i, as well as N (but not d) are varied. In order to do so, we will at first look for minimizers $[u, c_i]$ of $E_N[u, c_i]$ with fixed N. These, in turn, will be obtained by first calculating the extremals of E_N in (3.14) with fixed N. Such extremals are the phase-equilibria of the bar, which belong to separate branches in the space of admissible displacements ("u-space"); each branch is indexed by the number N of phase-boundaries, and is parametrized by d ("N-branches" of equilibria).

Extremals in an N-branch only give candidates for minimizers of the energy with fixed N and it is necessary to investigate separately the stability of each phase-equilibrium. After this is determined, total minimization of (3.13) is achieved by next considering competitors belonging to different N-branches, i.e. with a different number of transition points.

In order to study the stability of phase-equilibria, we take advantage of two features of our model: the convexity of f_+ and f_- and the description in terms of the transition points c_i. This, in fact, decouples for each N a relevant finite-dimensional part of

the problem where all the non-convexity is present, from the remaining infinite-dimensional setting in which the problem is convex. This decoupling has a clear physical meaning since the interfaces can be "frozen".

Owing to the convexity of f_+ and f_-, the displacement u can be minimized out of $E_N[u, c_i]$: doing so amounts to introducing, before actually considering phase-equilibria, another important class of configurations: the elastic equilibria of the bar. These are extremals of the energy (3.14) with the constraint that the position of the interfaces c_i be fixed in $[0, 1]$.

We will see that for given c_i, N, and d in their appropriate ranges, there exists a unique elastic equilibrium u_{d,c_i} (up to symmetries not affecting the energy), which the convexity hypotheses guarantee is the absolute minimizer of the energy against competitors with same N and c_i.

For each N, the displacement u can then be minimized out of E_N in (3.14), thereby obtaining $E_N^*(c_i, d)$, which describes the energy landscape of the bar in elastic equilibrium

$$E_N^*(c_i, d) = E_N[u_{d,c_i}, c_i], \quad \text{for} \quad N = 0, 1, \ldots. \tag{4.1}$$

The uniqueness of elastic equilibria implies that, for each N, E_N^* is a single-valued function of the imposed deformation and of the position of the interfaces.

The investigation of the stability properties of phase-equilibria belonging to an N-branch can now be done solely through the study of the minimizers of the functions E_N^*, $N = 0, 1, \ldots$, each of which just depends on a finite number of variables. Finding the extremals of $E_N[u_{c_i}, c_i]$ in the class of all elastic equilibria with variations of the points c_i (for fixed N), we obtain the functions $c_i(d)$ giving phase-equilibria as critical points of E_N^*, whose stability can then be assessed as usual. This allows us to eliminate the variables c_i from (4.1), so as to obtain the energy E_N^{**} of extremals as a function of d only. Indeed, denote by u_d the phase-equilibria belonging to an N-branch, and by $c_i(d)$ the equilibrium positions of the interfaces in u_d as functions of d; the phase-equilibrium energy of the bar in the elastic foundation is [see (3.14) and (4.1)]

$$E_N^{**}(d) = E_N^*(c_i(d), d) = E_N[u_d, c_i(d)], \quad \text{for} \quad N = 0, 1, \ldots. \tag{4.2}$$

Its d-derivative $\Sigma_N^{**}(d)$ gives the (phase-equilibrium) effective stress–strain relation of our system. For any given N, phase-equilibria at given d are, in general, and unlike elastic equilibria, not unique (nor are they always minimizers). Each N-branch of phase-equilibria thus splits in "sub-branches" with the same N; this in turn means that each N-branch of the phase-equilibrium energy E_N^{**} and of the stress–strain diagram will be multi-valued.

4.2. *Absolute minimization; phase diagram*

The final minimization of the energy now takes place among all the branches of E_N^{**}. Taking into account the presence of the physical parameters α and β, the absolute minimization now gives an integer-valued function $N(d, \alpha, \beta)$. In each appropriate region of (d, α, β)-space, $N(d, \alpha, \beta)$ indicates which one among the N-branches of solutions is the most stable (this constitutes the phase-diagram of the bar). By means

of $N(d, \alpha, \beta)$, the absolute-minimum energy of the bar is obtained as a single-valued function

$$E^{***}(d, \alpha, \beta) = E^{**}_{N(d,\alpha,\beta)}(d, \alpha, \beta); \tag{4.3}$$

its d-derivative $\Sigma^{***}(d, \alpha, \beta)$ gives the generalized Maxwell line in the stress–strain diagram $\Sigma^{**}_N(d)$.

Both functions $E^{**}_N(d)$ and $E^{***}(d)$ (and their first derivatives) will be referred to as the "macroscopic" or "effective" energy (and stress–strain relation) of the bar, related to its overall response (see Section 9). We stress that all the auxiliary functions introduced above, $E^{*}_N(c_i, d)$, $c_i(d)$, etc., also have an important role in the understanding of the phenomena connected with the mechanics of the multiphase bar, such as hysteresis, nucleation, etc.; an investigation of the properties of these functions is among our basic aims (see Section 8).

We also notice that it is quite common in the literature to use the phase fraction z of the bar (i.e. the length occupied by, say, the "$-$" component) as a major "macroscopic" variable [see for instance Cahn and Larché (1984), Khachaturyan (1983), Müller (1989), Abeyaratne *et al.* (1994)]. In most of the phenomenological models, a single-valued z-dependence of the energy is postulated rather than derived, based upon specific assumptions such as the incorporation of "coherence" or "interfacial" energy. In our case, the z-dependent equilibrium energy is obtained by defining by

$$E^{\#}(z, d) = \begin{cases} E^{\#}_0(z, d), \\ E^{\#}_1(z, d), \\ \quad \vdots \\ E^{\#}_N(z, d), \\ \quad \vdots \qquad (N = 0, 1, 2, \ldots) \end{cases} \tag{4.4}$$

where

$$E^{\#}_N(z, d) = E^{\#}_N(c_1 - c_0 + c_3 - c_2 + \ldots, d) = E^{*}_N(c_i, d) \tag{4.5}$$

for each N-branch. The description in terms of z does not distinguish between microstructures with different numbers of interfaces, therefore many details are lost, if compared to the description in terms of the internal parameters c_i. However, through our approach we see that even when using z as a variable, the energy $E^{\#}$ is multivalued, a fact not appreciated in the literature.

5. JUMP CONDITIONS

The elastic and phase-equilibria of the bar are obtained by piecing together smooth solutions of ODEs by means of suitable jump conditions at the transition points c_i, where a loss of smoothness does, in general, occur.

To find the explicit conditions for the extremals we use the results from the Appendix, applied to the energy function (3.14) of the bar. We obtain the following con-

ditions characterizing the phase-equilibria $[u, c_i]$ subject to the boundary conditions (3.15).

(i) The displacement u is necessarily at least class C^2 in $[0, 1]$, and in the intervals $[c_i, c_{i+1}]$, $i = 0, \ldots, N$, it satisfies the Euler–Lagrange equation [see (A.6)]

$$2\alpha u'''' - f''_{\pm}(u')u'' + 2\beta u = 0, \tag{5.1}$$

where the appropriate sign of $f''_{\pm}$ is taken in each interval.

(ii) At the transition points c_h the following must hold ($h = 1, \ldots, N$):

$$\begin{aligned} &[\![u'']\!]_{c_h} = 0 \quad \text{(balance of moments)}, \\ &[\![f'_{\pm}(u') - 2\alpha u''']\!]_{c_h} = 0 \quad \text{(balance of stresses, including couple stresses)}, \end{aligned} \tag{5.2}$$

and

$$[\![f_{\pm}(u')]\!]_{c_h} = 0 \quad \text{(Maxwell condition)}. \tag{5.3}$$

(iii) In addition to the imposed boundary conditions (3.15), the extremals must also satisfy

$$u''(0) = 0, \quad u''(1) = 0. \tag{5.4}$$

We recall the further jump conditions at the transition points that hold because all displacements are in C^1

$$[\![u']\!]_{c_h} = 0, \quad [\![u]\!]_{c_h} = 0 \quad \text{(smoothness conditions)}. \tag{5.5}$$

Conditions (5.1)–(5.5) and (3.15) characterize phase-equilibria. Notice that elastic equilibria do not necessarily satisfy the "Maxwell condition" (5.3); this means that in general there is a jump in energy at the transition points. Equation (5.3) is an explicit form of the critical-point condition for the "finite-dimensional" elastic energy E_N^* defined in (4.2)

$$\frac{\partial E_N^*}{\partial c_h} = -[\![f_{\pm}]\!]_{c_h} = 0. \tag{5.6}$$

The above equations for elastic equilibrium imply uniqueness of the solutions for given c_h (up to symmetry, see Section 6), as anticipated before (4.1). An interesting consequence of (5.3) is that our model shares the same extremals as the analogous model in which (3.1) is replaced by the function (2.19) considered in Section 2 [see Fig. 2(c)].

6. SYMMETRY

6.1. *Geometric symmetry ("G-symmetry")*

Denote by $[u_d, c_i(d)]$ any equilibrium solution, corresponding to the total strain d. The symmetric boundary conditions (3.15) introduce in the system a "geometric"

symmetry ("G-symmetry" for brevity). Indeed, by considering the displacement v_d and transition points $k_i(d)$ defined by

$$v_d(x) = -u_d(1-x), \quad \text{and} \quad k_i(d) = 1-c_{N-i+1}(d), \tag{6.1}$$

we see that $[v_d, k_i(d)]$ is another phase-equilibrium, in the same branch as $[u_d, c_i(d)]$ and with the same boundary conditions. In general, the G-related solutions v_d and u_d can be different, so that the G-symmetry can be a source of non-uniqueness in our system. However, it is not the only source: phase-equilibria are in general non-unique even up to symmetry; for instance, in addition to self-G-symmetric solutions, one can expect to find generic ones as well.

Now, referring to (3.13) and (3.15), we have

$$E[u_d, c_i(d)] = E[v_d, k_i(d)]; \tag{6.2}$$

for this reason, solutions generated by G-symmetry do not add any branching to the equilibrium energy function in (3.2) (or to the overall stress–strain diagram); in fact, sets of G-related equilibria in an N-branch of solutions simply "rerun" the same N-branch of the energy. The fact that there exists a G-image for any solution implies that the multi-valued functions $c_i(d)$, $c_i < c_{i+1}$, giving the phase-equilibrium positions of the phase-boundaries, satisfy

$$d(c_1, \ldots, c_N) = d(1-c_N, \ldots, 1-c_1), \tag{6.3}$$

where $d(c_i(d)) = d$. For the curve determined in (c_i, d)-space by the functions $c_i(d)$, this means invariance under mirror-symmetry across the plane parallel to the d-axis and through the diagonal of the domain $0 < c_i < c_{i+1} < 1$ on which the curve is defined.

Notice that the G-symmetry is destroyed if the non-symmetric boundary conditions (3.16) are considered, for in this case, the displacement defined by (6.1) no longer satisfies the imposed boundary conditions. Notice also that under (3.15), the G-symmetry is present in the system regardless of any assumptions about the energies in (3.1).

6.2. *Physical symmetry ("P-symmetry")*

Consider, as above, a phase-equilibrium $[u_d, c_i(d)]$, for given d. If we suppose that the two functions f_- and f_+ are such that

$$f_-(-u') = f_+(u'), \tag{6.4}$$

our system exhibits a further non-trivial "tension–compression" symmetry, which we will refer to as its "physical" symmetry ("P-symmetry" for brevity). If we define

$$v_{-d}(x) = -u_d(x), \quad k_i(-d) = c_i(d), \tag{6.5}$$

we find that under the hypothesis (6.4) $[v_{-d}, k_i(-d)]$ is also a phase-equilibrium, belonging to the same branch as $[u_d, c_i(d)]$ and corresponding to the boundary conditions given by $-d$. In v_{-d} the phases exchange the roles they had in u_d for each interval $[c_i, c_{i+1}]$, while the position of the phase-boundaries in the reference configuration remains the same. It is not difficult to verify that P-related solutions have

the same energy. The P-symmetry thus implies that the effective energy $E_N^{**}(d)$ introduced in (4.2) is an even function of d, as intuitively expected

$$E_N^{**}(d) = E_N^{**}(-d). \tag{6.6}$$

The same is true, of course, for the absolute-minimum energy $E^{***}(d)$. This symmetry also implies that the functions $c_i(d)$ satisfy

$$c_i(-d) = c_i(d), \tag{6.7}$$

so that the curve they generate in (d, c_i)-space is invariant under mirror-symmetry across the plane $(c_1, \ldots, c_N)$ (see Fig. 7 for the case $N = 2$). Clearly, the only self-P-symmetric solution is $u \equiv 0$ for $d = 0$.

Notice that the G- and P-symmetries are independent of each other. In the case of non-symmetric boundary conditions the P-symmetry, reflected in (6.6) and (6.7) still holds if the energies (3.1) satisfy (6.4); on the other hand, for energies such that (6.4) does not hold, the G-symmetry is still present if the symmetric boundary conditions (3.15) are considered (as is done in Sections 3–5).

Based on the above considerations, we can expect that in each N-branch of phase-equilibria with an even number N of transitions points there exists a sub-branch of self-G-symmetric extremals given by $[u_d, c_i(d)]$ such that

$$u_d(x) = -u_d(1-x), u_d(1/2) = u_d''(1/2) = 0, \quad c_i(d) = 1 - c_{N-i+1}(d). \tag{6.8}$$

The relations among the c_i indicate that in (c_i, d)-space the self-G-symmetric sub-branch always corresponds to a portion of the curve $c_i(d)$ belonging to the hyperplane $c_i = c_{N-i+1}$ through the diagonal of the region where the c_is are defined and parallel to the d-axis (see, for instance, Fig. 7 for $N = 2$).

7. THE CASE OF QUADRATIC ENERGIES

7.1. *Computation of the extremals*

From this point on, we concentrate on the most manageable case of quadratic energies, for which finding phase equilibria becomes an algebraic problem, and it is possible to calculate some exact solutions.

Let us assume that the non-dimensional energy density functions of both phases are symmetric parabolas ("bilinear material"):

$$f_\pm(u') = (u' \pm a)^2. \tag{7.1}$$

In (7.1) the elastic modulus is the same for both components, and a and $-a$ are strains giving the different stress-free stable equilibrium configurations for the two phases. The multi-valued energy (7.1) was originally suggested by Eshelby (1956) for the three-dimensional case, and has been widely used in the literature. Notice that the two parabolas satisfy (6.4); this introduces in the system the P-symmetry, besides the G-symmetry due to (3.15) (see Section 6). In what follows, we set $a = 1$.

Under (7.1), the Euler–Lagrange equation (5.1) that an extremal u must satisfy in each of the $N+1$ intervals $[c_i, c_{i+1}]$ becomes (the same for both phases)

$$\alpha u'''' - u'' + \beta u = 0; \tag{7.2}$$

while the jump conditions (4.2) and (4.5) at the transition points $c_i (i = 1, \ldots, N)$ are [see Truskinovsky (1994) for a dynamic generalization]

$$[\![u]\!]_{c_i} = 0, \quad [\![u']\!]_{c_i} = 0,$$
$$[\![u'']\!]_{c_i} = 0, \quad [\![\alpha u''' + 2\,\mathrm{sgn}(u')]\!] = 0. \tag{7.3}$$

Also, since the two energy parabolas (7.1) meet at $u' = 0$, the jump condition (5.3) is equivalent to

$$u'(c_i) = 0. \tag{7.4}$$

Notice that $(7.3)_4$ is obtained from (7.4), (5.2) and (7.1), because the jump in the classical contribution to the stress $f'_{\pm}(u') = 2(u' \pm a)$ at the points c_i is just equal to the jump in sign of the strain u'. Also recall the boundary conditions (3.15) and (5.4). Condition (7.4) shows that under hypothesis (7.1) phase-equilibria have their transition points at the zeros of the strain.

Since (7.2) can be solved explicitly, the infinite-dimensional part of the problem uncouples, and finding extremals reduces to the solution of a system of algebraic equations. This system of equations can be further decomposed into a linear and a nonlinear subsystem, reflecting the splitting of the energy into its convex (quadratic, in this case) and non-convex parts, as noticed earlier.

In each single-phase segment $[c_i, c_{i+1}]$ the equilibrium equation (7.2) is a 4th-order linear ODE with constant coefficients (known in the engineering practice as the equation of a flexible beam on an elastic foundation). The form of its solutions u depends on the sign of the quantity $1 - 4\alpha\beta$, and three cases should be distinguished.

(i) $1 - 4\alpha\beta > 0$:

$$u(x) = a_1 \exp(r_1 x) + a_2 \exp(r_2 x) + a_3 \exp(r_3 x) + a_4 \exp(r_4 x), \tag{7.5}$$

where

$$r_{1,2} = \pm\left[\frac{1 + (1 - 4\alpha\beta)^{1/2}}{2\alpha}\right]^{1/2}, \quad r_{3,4} = \pm\left[\frac{1 - (1 - 4\alpha\beta)^{1/2}}{2\alpha}\right]^{1/2}. \tag{7.6}$$

(ii) $1 - 4\alpha\beta = 0$:

$$u(x) = a_1 \exp(rx) + a_2 x \exp(rx) + a_3 \exp(-rx) + a_4 x \exp(-rx), \tag{7.7}$$

where

$$r = (2\alpha)^{-1/2} = (2\beta)^{1/2}. \tag{7.8}$$

(iii) $1 - 4\alpha\beta < 0$:

$$u(x) = \exp(r_1 x)[a_1 \cos(r_2 x) + a_2 x \sin(r_2 x)] + \exp(-r_1 x)[a_3 \cos(r_2 x) + a_4 x \sin(r_2 x)], \tag{7.9}$$

where

$$r_1 = \left[\frac{1}{4\alpha} + \left(\frac{\beta}{4\alpha}\right)^{1/2}\right]^{1/2}, \quad r_2 = \left[-\frac{1}{4\alpha} + \left(\frac{\beta}{4\alpha}\right)^{1/2}\right]^{1/2}. \tag{7.10}$$

Given c_i, the actual solutions in each single-phase interval $[c_i, c_{i+1}]$ are determined, and are matched at the transition points by means of the jump and boundary conditions $(7.3)_{1,4}$, (3.15) and (5.4). The phase-equilibrium values for the c_is are then obtained by using (7.4).

Now substitution of either one of the expressions (7.5), (7.7) or (7.9) into (7.3), (3.15) and (5.4), gives a linear system of $4(N+1)$ algebraic equations for $4(N+1)$ unknown constant coefficients $a_{h,i} = (a_{1,i}, a_{2,i}, a_{3,i}, a_{4,i})$, $i = 1, 2, \ldots, N$, appearing in the solution of (7.2) for each of the $N+1$ intervals $[c_i, c_{i+1}]$. For any generic choice of the parameters c_i the solutions to this linear system give the elastic equilibria of the bar. Explicitly, the case (i) of small α and β that we are mostly interested in, gives [see (7.5) and (7.6)]

$$\sum_{h=1}^{4} (a_{h,i} - a_{h,i-1}) \exp(r_h c_i) = 0, \quad i = 1, 2, \ldots, N,$$

$$\sum_{h=1}^{4} (a_{h,i} - a_{h,i-1}) r_h \exp(r_h c_i) = 0, \quad i = 1, 2, \ldots, N,$$

$$\sum_{h=1}^{4} (a_{h,i} - a_{h,i-1}) r_h^2 \exp(r_h c_i) = 0, \quad i = 1, 2, \ldots, N,$$

$$\sum_{h=1}^{4} (a_{h,i} - a_{h,i-1}) r_h^3 \exp(r_h c_i) = 2(-1)^i \alpha^{-1}, \quad i = 1, 2, \ldots, N,$$

$$\sum_{h=1}^{4} a_{h,0} = -d/2,$$

$$\sum_{h=1}^{4} a_{h,N} \exp(r_h) = d/2,$$

$$\sum_{h=1}^{4} a_{h,0} r_h^2 = 0,$$

$$\sum_{h=1}^{4} a_{h,N} r_h^2 \exp(r_h) = 0. \tag{7.11}$$

The solutions

$$a_{h,i} = a_{h,i}(c_1, \ldots, c_N; d, \alpha, \beta), \quad i = 1, 2, \ldots, N, h = 1, \ldots, 4, \tag{7.12}$$

of (7.11) completely determine the elastic equilibria. The coefficients $a_{h,i}$ and thus the elastic equilibria themselves, turn out to depend linearly on d.

The nonlinearity now is all concentrated in the problem of finding phase-equilibria, which amounts to solving the N nonlinear algebraic equations (7.4) with unknowns $c_1, \ldots, c_N$; explicitly

$$\sum_{h=1}^{4} a_{h,i}(c_1, \ldots, c_N; d, \alpha, \beta) r_h \exp(r_h c_i) = 0, \quad i = 1, 2, \ldots, N. \tag{7.13}$$

The functions

$$c_i = c_i(d, \alpha, \beta), \quad i = 1, 2, \ldots, N, \tag{7.14}$$

giving the solutions of (7.13), select, for each d, the phase-equilibrium values for the position of the transition points. In general, the solutions are non-unique so that (7.14) is multi-valued [see for instance (7.16) for the case $N = 1$].

We give two specific examples in which the solution (7.5) can be written in an explicit form. Elementary calculations provide the complete expression for the solutions constituting the 0-branch ($N = 0$) in u-space

$$u(x) = \frac{d}{4q}\left[(1+q)\left(\frac{\sinh(r_3 x)}{\sinh r_3} + \frac{\sinh(r_3(x-1))}{\sinh r_3}\right) - (1-q)\left(\frac{\sinh(r_1 x)}{\sinh r_1} + \frac{\sinh(r_1(x-1))}{\sinh r_1}\right)\right], \tag{7.15}$$

where r_1 and r_3 are defined in (7.6) and $q = (1-4\alpha\beta)^{1/2}$. In this case we have no internal variables (positions of the interfaces) and the problem is linear.

In the phase-equilibrium solutions belonging to the 1-branch ($N = 1$), there is one internal variable c for which the problem is nonlinear. Equation (7.13) in this case is given explicitly by

$$\begin{aligned} 0 = {} & r_1 b_1 \exp(cr_1)[1 + \exp(2r_1)\exp(-2cr_1)] \\ & - \frac{dr_1 r_3^2 \exp(r_1)\exp(-cr_1)}{2(r_3^2 - r_1^2)} \\ & + r_3 b_3 \exp(cr_3)[1 + \exp(2r_3)\exp(-2cr_3)] \\ & - \frac{dr_3 r_1^2 \exp(r_3)\exp(-cr_3)}{2(r_1^2 - r_3^2)}, \end{aligned} \tag{7.16}$$

where the coefficients b_1 and b_3 are

$$\begin{aligned} b_1 &= \frac{dr_1 r_3^2[\exp(r_1) + 1] + 2\alpha^{-1}[\exp(cr_1) - \exp(-cr_1)]}{2r_1[\exp(2r_1) - 1](r_3^2 - r_1^2)}, \\ b_3 &= \frac{dr_3 r_1^2[\exp(r_3) + 1] + 2\alpha^{-1}[\exp(cr_3) - \exp(-cr_3)]}{2r_3[\exp(2r_3) - 1](r_1^2 - r_3^2)}, \end{aligned} \tag{7.17}$$

Equation (7.16) provides the nonlinear c–d relation giving the position of the single interface c as an implicit multi-valued function of the imposed average strain d. Some of its properties will be discussed in the next Section (see Fig. 4).

We remark that one possibility to make the problem with a smooth, single-valued double-well energy [for instance (2.3)] more tractable, is to approximate the non-convex function by three parabolas: two downward and one upward in between, so

that the resulting function is smooth (continuous stress). In this case we obtain what is called a "trilinear material" and once again the problem can be reduced to an algebraic one and the analytical solution can be calculated. Obviously the displacement field in the trilinear model will be smoother than in the bilinear one, for example the third derivative of the displacements will be continuous.

8. THE SIMPLEST PHASE-EQUILIBRIA

In the previous sections we have defined, for each N, a branch of extremals of the functional (3.9) with boundary conditions (3.15) and energy (7.1) (phase-equilibria). In this section, by means of straightforward numerical computations based on the equations of Section 7, we investigate the main features of the simplest phase-equilibria. All the figures we present below correspond to the neighborhood of the origin in (α, β)-space, which is of most interest to us; the condition $1-4\alpha\beta > 0$ guarantees that all four characteristic roots of the Euler–Lagrange equation (7.2) are real and distinct [see (7.5) and (7.6)].

The main properties of the branches of extremals (parametrized by d in "u-space") will be presented through the analysis of the multi-valued functions $c_i(d)$ and $E_N^{**}(d)$ defined in (7.14) and (4.2). Recall the symmetry restrictions on the functions $c_i(d)$ and $E_N^{**}(d)$: (6.3) and (6.7) hold for $c_i(d)$, while (6.2) and (6.6) hold for $E_N^{**}(d)$. Thus the G-symmetry does not effect the equilibrium energy, while the P-symmetry makes it an even function of d.

While in the previous sections we focused on solutions meeting the boundary conditions (3.15), in this section we also present energy plots obtained from solutions to the non-symmetric problem (3.16). The computations are analogous and need not be reported here. Recall that the G-symmetry does not hold for the system with non-symmetric boundary conditions: in the energy plots this corresponds to a "doubling" of the sub-branches of each function $E_N^{**}(d)$ for fixed N. In fact, while the multiplicity of the solutions in u-space is the same for both cases, in the non-symmetric problem (3.16) relation (6.2) no longer holds: the sub-branches of minimizers that are no longer G-related do not reproduce the same energy sub-branch, and there is splitting in the energy diagrams.

8.1. *The 0-branch of phase-equilibria* (N = 0)

The phase-equilibria in the 0-branch are the extremals with no transition points: they constitute a family of non-homogeneous solutions of the linear equation (7.2) with boundary conditions (3.15) and (5.4), whose explicit expression is given by (7.15). The 0-branch is defined for all d, and for $d = 0$ it gives the homogeneous solution with identically zero displacements. In this case phase- and elastic equilibria coincide; they are unique for each d and are always stable against admissible competitors with no transition points. Uniqueness implies that each solution in the 0-branch is self-G-symmetric, so that relation (6.8) holds for all d. Solutions corresponding to boundary conditions given by d and $-d$ are P-related. Although there is a unique solution for each d in u-space, the energy $E_0^*(d) \equiv E_0^{**}(d)$ [see (4.1) and

(4.2)] is double-valued; its profile can be found in Fig. 3(a) (dashed line), where, however, only the lowest energy portion of each branch is shown. The corresponding effective stress–strain relation $\Sigma_0^{**}(d)$ is presented in Fig. 3(b) (dashed line).

Notice that the minima of $E_0^{**}(d)$ are always above zero; this happens due to the energy stored in the substratum. In the case of vanishing β (and arbitrary α), we obtain a family of homogeneous deformations whose energy profile reproduces the two original parabolas.

8.2. *The 1-branch of phase-equilibria* (N = *1*)

Extremals in the 1-branch have one transition point $c \in [0, 1]$; their explicit form is found by first solving (7.2) separately in $[0, c]$ and $[c, 1]$,and then "joining" the solutions at c, subject to the boundary conditions (3.15), (5.4), and jump conditions (7.3). This gives a linear system of eight equations with eight unknowns [see (7.11) for $N = 1$], which yields the elastic equilibria with one phase boundary.

The multi-valued function giving the position $c(d)$ for phase-equilibria is then defined implicitly by the single nonlinear equation (7.16) and (7.17); its plot in the (d, c)-plane for a specific choice of α and β is shown in Fig. 4, where the symmetries (6.3) and (6.7) have been used. The c–d relation determines the range in which the 1-branch exists: it is a bounded interval of the d-axis, unlike the 0-branch which is defined for any d. Also, the non-uniqueness of phase-equilibria in the 1-branch is clear from Fig. 4: each generic value of d in the existence domain gives four solutions which are pairwise G-related. Clearly, in this case, non-uniqueness is not generated completely by symmetry.

The 1-branch $E_1^{**}(d)$ is represented in Fig. 3(a) by the triangular curve (chain-dot dashed line), which, due to (6.2), is "run over" twice by the two G-related sub-branches of minimizers. For this reason, the four equilibria shown in Fig. 4 for each d, give only two points on the 1-branch of the energy in Fig. 3(a). For vanishing α and β the lower side of the triangle follows the convex envelope of the original parabolas and in this way the single-interface solutions contribute to Ericksen's non-uniqueness.

Now Fig. 3(a) can be compared with Fig. 5 where the energies $E_N^{**}(d)$ corresponding to the non-symmetric boundary conditions (3.16) are shown for $N = 0, 1, 2$. Although the qualitative structure of the c–d diagram is the same in both cases, the sub-branches of $E_1^{**}(d)$ in Fig. 5 (dashed line) are no longer superimposed and the expected splitting occurs. Notice that the P-symmetry still holds so that due to (6.6), the energy is even in both Fig. 3(a) and Fig. 5.

According to Fig. 4, we have $c = 0$ and $c = 1$ at $d = 0$; thus the 1-branch intersects the 0-branch in u-space exactly at the trivial homogeneous solution $u \equiv 0$ (this is shown in Fig. 6, which pictures the complete topological structure of the simplest branches of extremals in the infinite-dimensional u-space represented as the three-dimensional space). Clearly, moving away from the solution $u \equiv 0$ (for $d = 0$) along the 1-branch entails the creation and growth of an infinitesimal nucleus of new phase from one of the ends of the bar, without overcoming an energy barrier ("second order transition").

Notice that $u \equiv 0$ is the only common point of intersection of all branches of

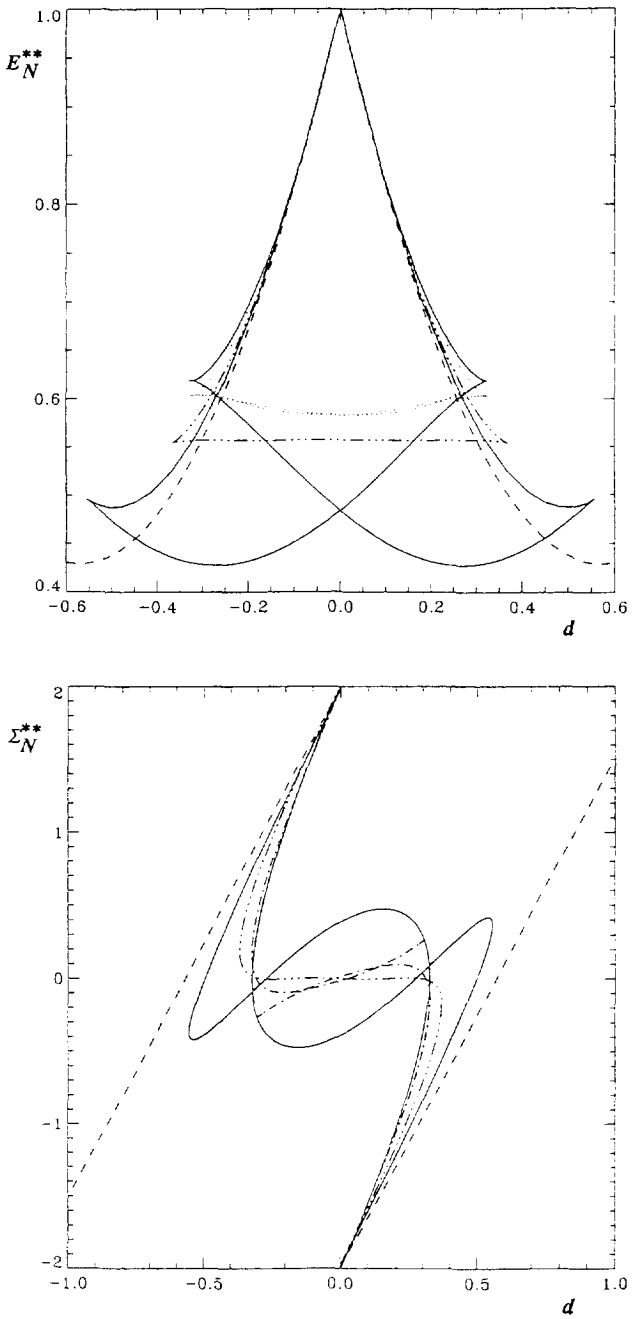

Fig. 3. (a) The calculated N-branches of the effective energy $E_N^{**}(d)$ for the case of symmetric boundary conditions (3.15) for $\alpha = 0.01$ and $\beta = 10$; – – – $N = 0$; – · · · – $N = 1$; —— $N = 2$, self-G-symmetric sub-branch; · · · $N = 2$, non-self-G-symmetric sub-branch. (b) The branches in the effective stress–strain curves $\Sigma_N^{**}(d)$ corresponding to the effective energy branches shown in (a). – – – $N = 0$; – · · · – $N = 1$; —— $N = 2$, self-G-symmetric sub-branch; – · – · – $N = 2$, non-self-G-symmetric sub-branch.

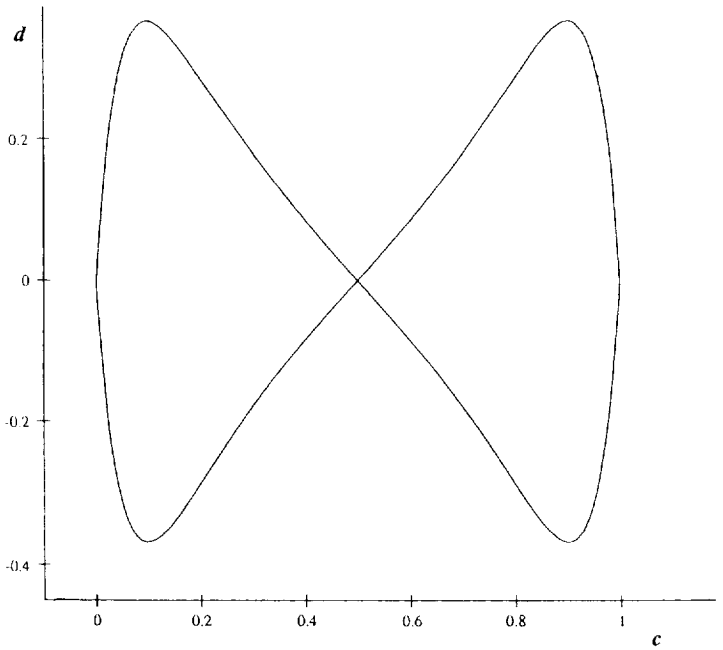

Fig. 4. The curve showing the relation between the imposed overall strain d and the position of the interface c for the 1-branch of extremals ($\alpha = 0.01, \beta = 10$); both the G- and P-symmetries are taken into account. The lack of one-to-one correspondence between d and c indicates the multiplicity of the one-interface equilibria for given d.

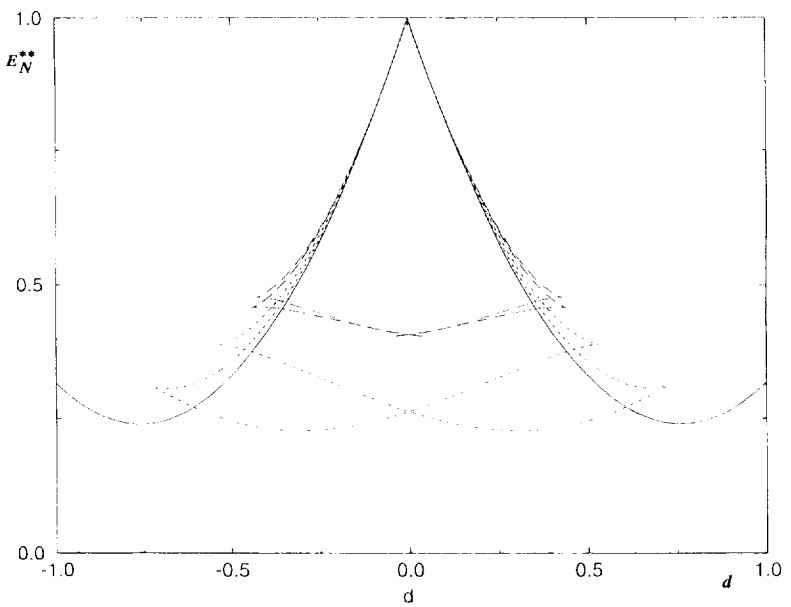

Fig. 5. The same N-branches of the effective energy $E_N^{**}(d)$ as in Fig. 3(a) for the case of non-symmetric boundary conditions (3.16) for $\alpha = 0.01$ and $\beta = 1$; ——— $N = 0$; - - - $N = 1$; — · — · — $N = 2$.

extremals in u-space which implies that all the energy branches meet at $d = 0$, as shown in Fig. 3(a) for $N = 0, 1, 2$. This is due to the absence of the spinodal region in the energy (7.1). In the case of the smooth double-well energy (2.3) with a spinodal region the bifurcation diagram similar to the one shown in Fig. 3(a) will be less singular around the point $d = 0$. In particular when $\beta = 0$, the quadrature solutions are available in both models; one can show that for the model based on (2.3), the branch of the effective energy corresponding to the monotone extremals [the analog of our $E_1^{**}(d)$] has a triangular shape similar to the 1-branch shown in Fig. 3(a). However, it bifurcates from the homogeneous branch of the effective energy [the analog of our $E_0^{**}(d)$] and then reconnects with it in two different points rather than in one point ($d = 0$), as in our case.

The 0- and 1-energy branches intersect at points other than $d = 0$; however, this does not mean that the corresponding branches of extremals intersect in u-space. For instance consider the points where intersection occurs between these two energy branches. At these points the different extremals are in fact physically apart (distant in u-space, see Fig. 6), and there are energy barriers between them that cannot be read from the effective energy diagram (notice, however, the stress drops at those points in the effective stress–strain diagram). The system passing from one equilibrium to the other (for $d \neq 0$) reflects the phenomenon of finite nucleation at the ends of the bar. We recall that in our model nucleation without overcoming an energy barrier is possible only at $d = 0$.

By considering for each d the elastic equilibrium energy $E_1^*(c, d)$ [see (4.1)], one can show that the phase-equilibria giving the lower side of the energy triangle $E_1^{**}(d)$ in Fig. 3(a) (chain-dot dashed line) are all stable, for they are local minima of $E_1^*(c, d)$ as a function of c for fixed d. The two other branches (upper sides of the triangle) are unstable because they correspond to local maxima of $E_1^*(c, d)$ (saddle points in u-space). This is again summarized in Fig. 6, where the "double loop" depicting the 1-branch of extremals is shown with its stable portions represented by a solid line.

8.3. *The 2-branch of phase-equilibria* (N = 2)

Extremals on the 2-branch have two transition points c_1 and c_2. In this case the elastic equilibria are obtained from the system of 12 linear equations (7.11) which gives 12 coefficients $a_{h,i} (i = 1, 2, 3; h = 1, \ldots, 4)$. Phase-equilibria are then determined from the solution of two non-linear equations (7.13) providing two (multi-valued) functions $c_1(d)$ and $c_2(d)$, whose generic plot is presented in Fig. 7.

The essential structure of the bifurcation diagram in (d, c_1, c_2)-space (when the G-symmetry is taken into account, but not the P-symmetry) can be observed. The branch of the curve which stays on the plane $c_2 = 1 - c_1$, corresponds to the self-G-symmetric extremals which are typical in the case of even N [see (6.8)]. Two G-related sub-branches of non-self-G-symmetric equilibria bifurcate from the self-G-symmetric sub-branch with no energy barrier. On the other hand, intersection of energy sub-branches with different N (for instance with $N = 0$ and $N = 2$) corresponds to finite nucleation in the interior of the bar, for which there exists an energy barrier.

It follows from Fig. 7 that the solutions belonging to the 2-branch exist on a bounded interval of the d-axis. Also their number can be determined from Fig. 7,

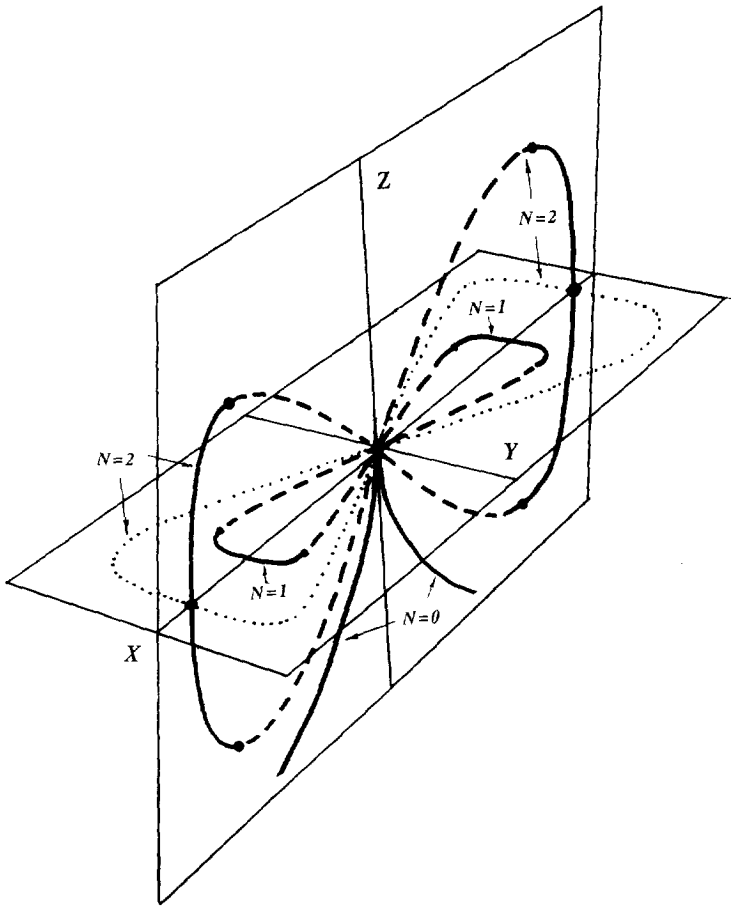

Fig. 6. Generic topological structure of the bifurcation diagram for the 0-, 1- and 2-branches of extremals in u-space in the case of a system with no symmetries. Stable equilibria are indicated by solid lines, unstable equilibria by dashed or dotted lines. When the symmetric boundary conditions (3.15) and symmetric energy (7.1) are considered, the G- and P-symmetries can be represented here by reflection across the (Z, X)-plane and reflection across the (Z, Y)-plane, respectively (for example, self-G-symmetric solutions belong to the (Z, X)-plane). In this case the common "point" where all branches meet corresponds to the trivial solution $u \equiv 0$. In this figure the count of equilibria for given d is not immediate because d is not a "single-valued" parameter on the branches.

taking into account that the curve must be symmetrized by means of a reflection across the (c_1, c_2)-plane [see (6.7)]. For generic d near 0 there are up to 10 solutions, and their number decreases to 2 farther away from 0. This can also be seen from the plot of the 2-branch of the equilibrium energy $E_2^{**}(d)$ shown in Fig. 3(a). The multi-valued function $E_2^{**}(d)$ is composed of roughly triangular branches (solid lines) corresponding to the self-G-symmetric solutions, with bifurcating sub-branches (dotted lines) corresponding to the non-symmetric solutions. The function $E_2^{**}(d)$ is even due to P-symmetry, and its sub-branches corresponding to non-self-G-symmetric extremals are run over twice by the G-related solutions in u-space.

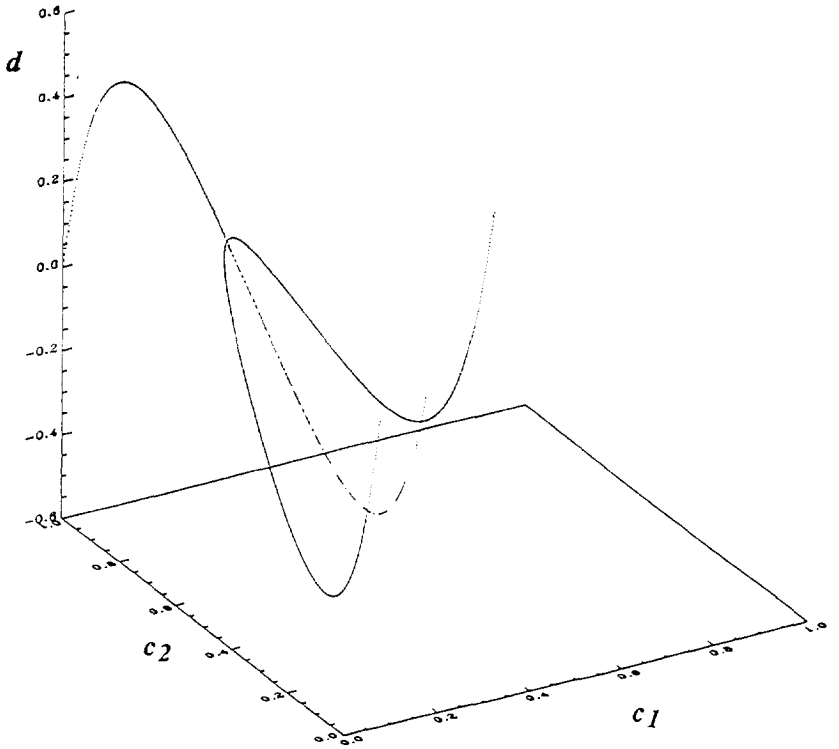

Fig. 7. The phase equilibrium curve in (c_1, c_2, d)-space for the 2-branch of extremals. For clarity, the part of the curve generated by P-symmetry (corresponding to mirror symmetry across the (c_1, c_2)-plane) is omitted. The main branch, which stays in the plane $c_2 = 1 - c_1$, corresponds to self-G-symmetric extremals; the two side branches correspond to G-related non-symmetric solutions ("twins").

At $d = 0$ all sub-branches of $E_2^{**}(d)$ meet at the trivial solution. As follows from Fig. 3(a), for $d = 0$ we also obtain solutions which have lower energy than the trivial one; the self-G-symmetric solution which has the lowest-energy, is close to being periodic near $d = 0$. We have no proof that this solution actually corresponds to the global minimum of our functional, however the preliminary numerical calculations of Collins for $N = 1 \div 6$ strongly suggest that this is the case for our choice of α and β. From the analysis of Müller (1993) we only know that (for a smooth two-well energy density) in the limit of small α and for $\beta = 1$, the global minimum of the energy for $d = 0$ is attained by a self-G-symmetric periodic function, with $N \sim \alpha^{-1/6}$. From our investigation of the local minimizers, we expect that also for the global minimizer periodicity will be lost away from $d = 0$ (at least near the ends of the bar), while self-G-symmetry remains.

We also remark that in our examples the non-self-G-symmetric sub-branches always have higher energy than the lowest-energy portion of the self-G-symmetric sub-branch. Their stability can be assessed from the analysis of the function $E_2^*(c_1, c_2, d)$ for fixed d. It is possible to show that the lowest energy portion of the symmetric sub-branch is stable, i.e. the corresponding solutions are minima of $E_2^*(c_1, c_2, d)$. All the

other extremals corresponding to maxima or saddle points of $E_2^*(c_1, c_2, d)$ (all are saddle points in u-space) are unstable phase-equilibria. In particular, the G-related non-symmetric extremals (twins) are unstable (this is also indicated in Fig. 6). The fact that, as is the case of $N = 1$ and 2, only the lowest energy portion of each sub-branch corresponds to physically relevant states (at least metastable) that might be generic.

In Fig. 5 the effective energy function $E_2^{**}(d)$ is also shown for the case of the non-symmetric boundary conditions (3.16). Notice that unlike Fig. 3(a) $E_2^{**}(d)$ in Fig. 5 lies above $E_1^{**}(d)$ for all (d).

9. CONCLUSIONS

Although our investigation is still preliminary, and most of the issues are left for more detailed study, we can make a number of interesting observations which we summarize in this final section.

(1) In the various one-dimensional models which extend Ericksen's earlier analysis but neglect surface energy, the energy infimum as a function of total strain is the convex envelope of the original phase energy densities and one observes infinite refinement of the microstructures. In our case, when a strain-gradient term is considered in the energy, finite-scale microstructures (rather than infinitely fine ones) occur as minimizers. One can expect that at equilibrium, the macroscopic energy in the system with surface energy is higher than in the equivalent system without surface energy. That means the plot of the total energy of the bar lies above the convex envelope of the two-well energy, with a loss of convexity for the effective energy (the corresponding effects in three dimensions would cause a similar deviation from the quasiconvex envelope). Our examples show, however, that the overall energy function is at least locally convex (elliptic), at the expense of reduced smoothness [see Fig. 8(a)]. Smoothness is lost as the system switches from one branch to another of the effective energy (7.2). The corresponding effective stress–strain relation is therefore a curve that is only piecewise continuous, with "jumps" and (locally) non-negative moduli [see Fig. 8(b)].

The above considerations imply a distinct "quantization" effect in the continuous system, not to be confused with the discreteness in the system of snap-springs [see Müller and Villaggio (1979) and Fedelich and Zanzotto (1992)]. We stress that this non-smoothness in the absolute-minimum energy is not an artificial effect introduced in the model *ab initio*, for it is not due to the "corner" in the original energy [see Fig. 2(b, c)] but, rather is a result of the branching of the minimizers, and may be expected in models with a smooth energy (and spinodal region) as well. Such branching can generate (non-smooth) oscillations also in the z-dependent absolute-minimum energy obtained from (4.4). This means that the jumps in the Maxwell line are in fact intrinsic also to smooth models; this gives a possible interpretation for the wiggles that are observed in yield and recovery lines in the (quasistatic) uniaxial tension experiments on bars made of multiphase shape-memory alloy [see, for instance, Müller and Hu (1991)]. We also recall that the jumps in stress reflect the transitions between separate

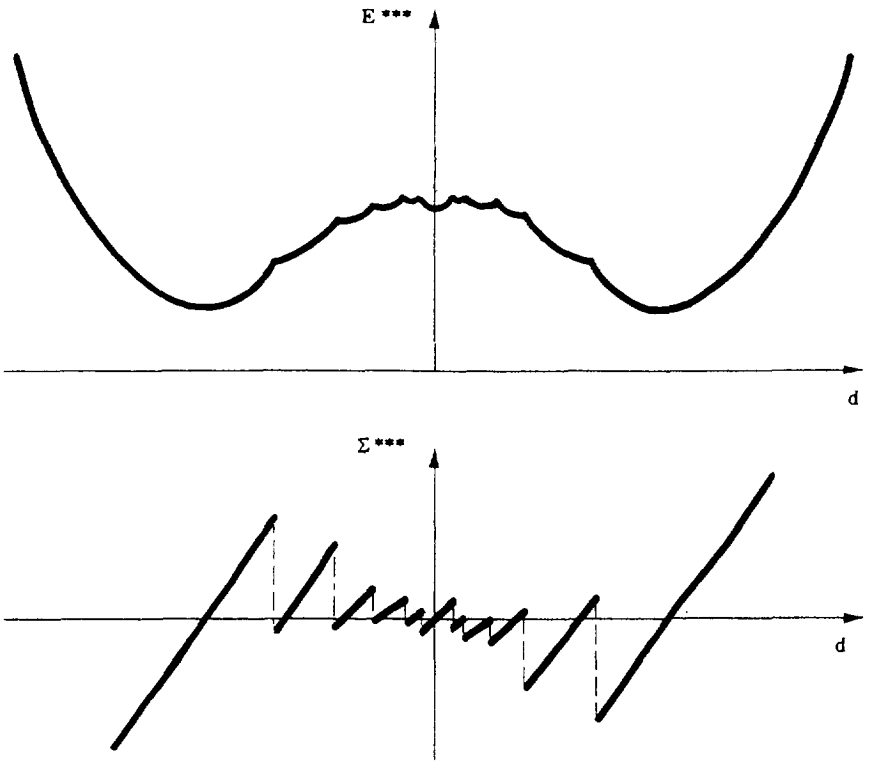

Fig. 8. Maxwell construction for sufficiently small α and β. (a) Absolute-minimum energy $E^{***}(d, \alpha, \beta)$ with non-smooth oscillations. (b) The saw-like discontinuous Maxwell line $\Sigma^{***}(d, \alpha, \beta)$ in the overall stress–strain diagram.

(and possibly distant) branches of equilibria, with energy barriers in between; their closeness in energy is misleading, and following the energy envelope in fact implies a sequence of finite nucleation events. The estimate of such energy barriers will be one of the important steps in the understanding of the actual evolution of the phase transitions under changing boundary conditions. Notice also that the effective energy is not constitutive, but is sample (size)-dependent [through (3.8)].

(2) The augmentation of the original bar problem provides one way of obtaining a selection criterion among the non-unique solutions found by Ericksen. In our model the number of interfaces N is given by the function $N = N(d, \alpha, \beta)$ defined in Section 4. Our examples with low N suggest that extensive numerical computations are needed to obtain a thorough description of the phase diagram in (d, α, β)-space; however, its structure in the vicinity of the point $\alpha = 0$, $\beta = 0$ (for large N and $d = 0$) is given by the parabolas (2.17).

For the purpose of obtaining a selection criterion, which is of particular interest, only these asymptotics are relevant: recall that for N large, in the limit for vanishing α and β, N depends only on $\gamma = \beta\alpha^{-1/2}$. Thus the ratio γ is the only essential factor in the selection of the most energetically preferable solution among the different equilibrium configurations indicated by Ericksen. This is a "ghost" that determines the number

of interfaces. We also notice that in the bar there is a tendency towards coarsening or refinement of a microstructure depending on whether solutions with smaller N or larger N are more energetically favorable. This is decided, in general by the values of α and β (and by γ in Ericksen's case). For instance, coarsening is energetically preferred in the regions where α is large, and this is of interest in connection to what in physics is called a "size effect". Observations show that when the particles undergoing phase transition are sufficiently small, configurations with very few twin bands or no bands at all are preferred to microstructures with many interfaces (Monzen *et al.*, 1989). In our model, this phenomenon is due to the fact that when L is small, α is large [see (3.8)]. In the corresponding part of the phase diagram, refinement of the microstructures is energetically unfavourable, and a coarsening effect is thus expected. We also notice that although this has not been proved in the preceding sections, there are ranges of the parameters α and β in which the solutions with low N that we have explicitly calculated (see Section 8) are the absolute minimizers rather than mere relative minimizers. What is shown in our figures (see Section 8) is thus the relevant part of the macroscopic energy for a small particle. This is, of course, not the case for large "bars" for which refinement is clearly energetically favorable.

In Fig. 9(a) and (b) we separately show the schematic dependence of N on the overall imposed strain d, and on the size of the sample L. The N–d relation shows that N grows to a maximum and then decreases as d is increased. A similar dependence was observed in experiments on shape-memory single crystals during uniaxial tension tests by Fu *et al.* (1992). Analogously, the N–L relation depicted in Fig. 9(b) can be connected to the work of Kato *et al.* (1977), who experimentally determined a "staircase" in the relation between the particle size and the number of the bands in nanometer-size particles. Staircases of this kind are also known in the systems with competing spatial interactions studied in physics [ANNNI model, F–K model; see for instance Selke (1994)].

(3) The previous analysis shows that after minimizing out the elastic fields, the

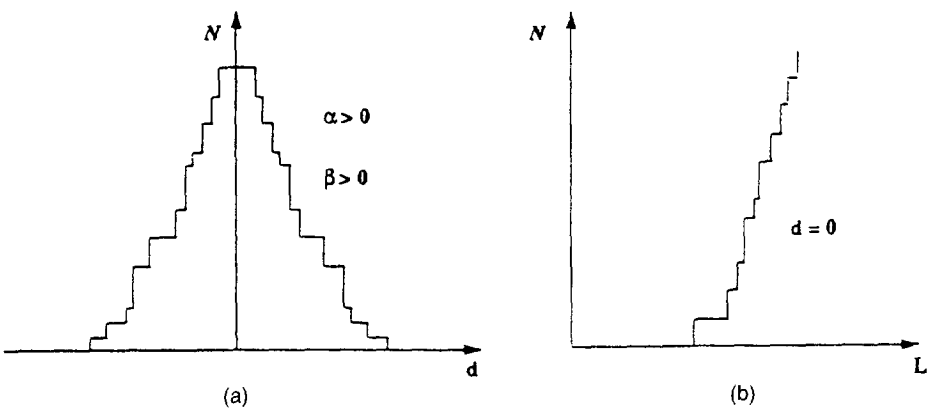

Fig. 9. The optimal number N of interfaces as a function of different parameters. (a) The function $N(d, \alpha, \beta)$ for given α and β; (b) the function $N(L) = N(0, \alpha, \beta)$ for given β and $\alpha \sim L^{-2}$, where L is the size of the sample.

energy of an N-branch of equilibria, as a function of the positions of the interfaces, exhibits multiple local extrema, and different minima correspond to different local minimizers in u-space, moreover their number dramatically increases with N. The energy can thus be viewed as having multiple macro-oscillations (wiggles). On the other hand, it is well known (Roitburd, 1978; Ball and James, 1992) that in more realistic three-dimensional models even more complicated multilayered configurations are common and are indeed observed experimentally [see, for instance, Tan and Xu (1990)]. Each next level of microstructure (possibly involving more than two wells in the original energy density of the material) affects the energy by the same mechanism as we discuss here, and this produces extra meso-oscillations of a finer scale in the effective potential; indeed, there may be several internal sub-levels of microstructure and thus several sub-levels of oscillations in the energy. This effect should ultimately be responsible, for instance, for such phenomena as the "locking-in" of elastic equilibria considered in the previous sections. Finally, at microlevel (the level of the lattice) the energy as a function of the positions of the interfaces has micro-oscillations represented by, say, Pieerls barriers. The fact that energy curves with various internal scales of oscillations should be considered (also in relation to some macroscopic aspects of the behavior of bodies) has only recently been appreciated in the literature. For example, oscillations (wiggles) are added *ad hoc* by Abeyaratne *et al.* (1994) to the z-dependent effective energy function, based on the experimental analysis of the "tip-splitting" mechanism for twin layers, which appears to be among the key elements in their model for the hysteretic behavior observed in biaxial stretching tests on shape-memory alloys.

(4) The results of this investigation may help to clarify the experimental observations regarding hysteresis. It is reasonable to relate hysteresis to the possibility that the system gets locked in metastable equilibria, and we concentrate in this paper on their detailed analysis. However, in order to account properly for hysteresis, a model for dynamics is of course necessary. Two directions can be taken: full-scale PDE analysis or constrained dynamics in a finite dimensional subspace of internal parameters. In the first case one adds to our Euler–Lagrange equation the standard u_{tt} term originating from kinetic energy and the dissipative term, say, u_{xxt} if the mechanism of dissipation is (Kelvin) viscosity (see Truskinovsky, 1993). In the absence of the surface energy term, this model has been studied by Ball *et al.* (1991). The second possibility is to assume the elastic equilibration to be instantaneous (fast mode), relating dynamics to the quasistatic migration of phase boundaries (phase-equilibration, slow modes). In this case the simplest approach to the dynamics in c-space may be gradient flow, for which our model, with the elastic fields minimized out, provides the relevant potential. The corresponding system of ODE in the case of "wiggly enough" potential is known to describe locking phenomena (Abeyaratne *et al.*, 1994). Notice that the potential wells created by "meso-oscillations" (which this model does not take into account) could make elastic equilibria at least metastable, and this might be of importance for the interpretation of the recent experimental tests exploring the interior of the hysteresis loop by Fu *et al.* (1992) and Ortín (1992). The fact that internal loops reproduce themselves at different scales (Ortín, 1992) may be a reflection of the existence of several levels of oscillations in the effective energy as discussed above.

ACKNOWLEDGEMENTS

We would like to acknowledge the help of A. Polyakov and K. Hane with the numerical computations that led to many of the figures presented in this paper, and D. Schryvers for providing the original micrograph shown in Fig. 1. We appreciate helpful discussions with G. Barenblatt, M. Lanza de Cristoforis, S. Müller, A. Vainstein and J. Willis and we thank the Italian CNR, as well as AFOSR (AFOSR-91-0301), NSF (NSF/DMS-8718881), ARO (DAAL 03-92-G-003) and ONR (N00014-91-J-4034), for partial financial support. Finally, we would like to thank each other's institutions for the warm hospitality provided during much of our work.

REFERENCES

Abeyaratne, R., Chu, C. and James, R. D. (1994) Kinetics and hysteresis in martensitic single crystals. In *Proc. Symposium on the Mechanics of Phase Transformations and Shape-Memory Alloys*, ASME, to appear.

Ball, J. M., Holmes, P. J., James, R. D., Pego, R. L. and Swart, P. J. (1991) On the dynamics of the fine structure. *J. Nonlin. Sci.* **1,** 17–70.

Ball, J. M. and James, R. D. (1992) Proposed experimental test of a theory of fine microstructure and the two-well problem. *Phil. Trans. Royal Soc. Lond. A* **338,** 389–450.

Ball, J. M., Chu, C. and James, R. D. (1994) Metastability of martensite, in preparation.

Barenblatt, G. I. (1995) *Similarity, Self-Similarity and Intermediate Asymptotics.* Cambridge University Press, Cambridge.

Bhattacharya, K., James, R. D. and Swart, P. J. (1994) A nonlinear dynamic model for twin relaxation with applications to Au–Cd and other shape-memory alloys, in preparation.

Brandon, D. and Rogers, R. C. (1994) Nonlocal regularization of L. C. Young's tacking problem. *Appl. Math. Optimiz.* **25,** 287–306.

Cahn, J. W. and Larché, F. (1984) A simple model for coherent equilibrium. *Acta Metall. Mater.* **32,** 1915–1923.

Carr, J., Gurtin, M. E. and Slemrod, M. (1984) Structured phase transitions on a finite interval. *Arch. Rat. Mech. Anal.* **86,** 317–351.

Ericksen, J. L. (1975) Equilibrium of bars. *J. Elasticity* **5,** 191–202.

Ericksen, J. L. (1977) Special topics in elastostatics. *Advances in Applied Mechanics*, pp. 189–244. Academic Press.

Eshelby, J. D. (1956) The continuum theory of lattice defects. *Solid State Phys.* **3,** 79–144.

Fedelich, B. and Zanzotto, G. (1992) Hysteresis in discrete systems of possibly interacting elements with a two-well energy. *J. Nonlin. Sci.* **2,** 319–342.

Fosdick, R. L. and Mason, D. E. (1994) Single phase energy minimizers for materials with nonlocal spatial dependence. IMA Preprint 1212, Minneapolis, Minnesota, U.S.A. (*Quart. Appl. Math.*, to appear).

Friesecke, G. and McLeod, J. B. (1994) Dynamics as a mechanism preventing the formation of finer and finer microstructure. *Arch. Rat. Mech. Anal.*, to appear.

Fu, S., Müller, I. and Xu, H. (1992) The interior of the pseudoelastic hysteresis. *Mater. Res. Soc. Symp. Proc.* **246,** 39–42.

Graff, M., Scheidl, R., Troger, H. and Weinmüller, E. (1985) An investigation of the complete post-buckling behaviour of axisymmetric spherical shells. *ZAMP* **36,** 123–134.

James, R. D. (1992) Deformation of shape-memory materials. *Mater. Res. Soc. Symp. Proc.* **246,** 81–90.

Kaganova, I. and Roitburd, A. (1987) Equilibrium shape of an inclusion in a solid. *Sov. Phys. Dokl.* **32,** 925–927.

Kato, M., Monzen, R. and Mori, T. (1977) A stress-induced martensitic transformation of spherical iron particles in a Cu–Fe alloy. *Acta Metall.* **26,** 605–613.

Kelly, A. and Groves, G. W. (1970) *Crystallography and Crystal Defects.* Harlow, Longmans.

Khachaturyan, A. G. (1983) *Theory of Structural Transformations in Solids*. John Wiley and Sons, New York.
Kinderlehrer, D. and Ma, L. (1994) The hysteretic event in the computation of magnetization and magnetostriction. In *Proc. Nonlinear Differential Equations and their Application*. (ed. H. Brezis and J.-L. Lions). Collège de France Sem., to appear.
Kohn, R. and Müller, S. (1992) Branching of twins near an austenite-twinned-martensite interface. *Phil Mag. A.* **66,** 697–715.
Lifshitz, I. M. (1948) Macroscopic description of twinning phenomena in crystals. *Sov. Phys. JETP* **18,** 1134–1152.
Monzen, R., Kato, M. and Mori, T. (1989) Diffusional relaxation around martensitically transformed Fe–Co particles in a Cu matrix. *Acta Metall. Mater.* **37,** 3177–3182.
Müller, I. (1989) On the size of hysteresis in pseudoelasticity. *Cont. Mech. Thermodyn.* **1,** 125–142.
Müller, I. and Villaggio, P. (1977) A model for an elastic-plastic body. *Arch. Rat. Mech. Anal.* **65,** 25–46.
Müller, I. and Xu, H. (1991) On the pseudo-elastic hysteresis. *Acta Metall. Mater.* **39,** 263–271.
Müller, S. (1990) Minimizing sequences for nonconvex functionals, phase transitions and singular perturbations. In *Problems Involving Change of Type* (ed. Kirchgässner), Lecture Notes in Physics, Vol. **359,** pp. 31–44. Springer, Berlin.
Müller, S. (1993) Singular perturbation as a selection criterion for periodic minimizing sequences. *Calculus of Variations* **1,** 169–204.
Ortín, J. (1992) Preisach modeling of hysteresis for a pseudoelastic Cu–Zn–Al single crystal. *J. Appl. Phys.* **71,** 1454–1461.
Parry, G. P. (1987) On internal variables models of phase transitions. *J. Elasticity* **17,** 63–70.
Parry, G. P. (1989) Stable periodic phase boundaries in unloaded crystals. *Cont. Mech. Thermodyn.* **1,** 305–314.
Roitburd, A. L. (1978) Martensitic transformation as a typical phase transformation in solids. *Solid State Phys.* **33,** 317–390.
Rosakis, P. (1992) Compact zones of shear transformation in an anisotropic solid. *J. Mech. Phys. Solids* **40,** 1163–1195.
Schryvers, D., Ma, Y., Toth, L. and Tanner, L. (1994) Electron microscopy study of the formation of Ni_5Al_3 in a $Ni_{62.5}Al_{37.5}$ alloy. II: Plate crystallography. *Acta Metall. Mater.*, in press.
Selke, W. (1994) Spatially modulated structures in systems with competing interactions. *Phase Transitions and Critical Phenomena* (ed. C. Domb and J. L. Lebovitz). Academic Press, in print.
Tan,S. and Xu, H. (1990) Observations in CuAlNi single crystal. *Cont. Mech. Thermodyn.* **2,** 241–244.
Truskinovsky, L. (1993) Kinks versus shocks. In *Shock Induced Transitions and Phase Structures in General Media* (ed. R. Fosdick, E. Dunn and M. Slemrod), IMA Vol. **52,** pp. 185–229. Springer-Verlag.
Truskinovsky, L. (1994) About the 'normal growth' approximation in the dynamical theory of phase transitions. *Cont. Mech. Thermodyn.* **6,** 185–208.
Truskinovsky, L. and Zanzotto, G. (1995) Finite-scale microstructures and metastability in one-dimensional elasticity. *Meccanica* **30,** 577–589.
Young, L. C. (1980) Lectures on the calculus of variations and optimal control theory, Chelsea, New York.

APPENDIX: CALCULUS OF VARIATIONS

In this Appendix we obtain the jump conditions indicated in Section 5. We will use some classical arguments applied to the general functional

$$\Lambda_N[u, c_1, \ldots, c_N] = \sum_{i=0}^{N} \int_{c_i}^{c_{i+1}} L_\pm(x, u, u', u'')dx. \tag{A.1}$$

In (A.1) the Lagrangian $L_\pm$ can be multi-valued with branches L_+ and L_- that are smooth, convex functions of their arguments. The energy (3.14) of our bar is a special case of (A.1). The same convention as for (3.14) holds: L_- or L_+ must be taken alternately in the integrand for each interval $[c_i, c_{i+1}]$.

Let us consider a candidate extremal $[u, c_i]$ for (A.1), and recall that in Section 3 we have limited ourselves to displacement fields that are C^1, piecewise C^2, in $[0, 1]$. We will assume more regularity for u, and suppose it to be smooth enough so as to let us perform all the necessary operations, with discontinuities of its higher derivatives occurring at most at the transition points c_i. For example, in the specific case of the energy functional (3.12) of the bar, u is required to be C^1, piecewise C^4 in $[0, 1]$.

In order to test $[u, c_i]$ under the boundary conditions (3.15), we fix N and d, and consider [see Ericksen (1977)] the one-parameter family of admissible variations, for both dependent and independent variables, defined by

$$X = X(x, \varepsilon), \quad u = u(X, \varepsilon), \tag{A.2}$$

with

$$X(x, 0) = x, \quad u(x, 0) = u(x), \tag{A.3}$$

and boundary conditions

$$X(0, \varepsilon) = 0, \quad X(1, \varepsilon) = 1, \quad u(0, \varepsilon) = -d/2, \quad u(1, \varepsilon) = d/2. \tag{A.4}$$

According to $(A.2)_1$ the positions of the new transition points C_i in $[0, 1]$ are

$$C_i = X(c_i, \varepsilon), \quad \text{for} \quad i = 1, \ldots, N. \tag{A.5}$$

We assume that $(A.2)_1$ is of class C^2, and, of course, that it leaves the constraint $C_i < C_{i+1}$ satisfied. The fields $(A.2)_2$ describe competitors with fixed N that are non-equilibrium states of the bar, with fixed ends and displaced positions of the phase-boundaries. We will require that they be at least of class C^1, piecewise C^2, but will discuss in detail below how different choices of the variations lead to different equilibrium conditions. We define, as usual, the variations $\delta = [\partial/\partial\varepsilon]_{\varepsilon=0}$ and $\Delta = [d/d\varepsilon]_{\varepsilon=0}$ for any quantity that depends on ε. Then, by $(A.2)_{1,2}$, we have $\Delta u = \delta u + u'\delta X$, and the following commutation relations hold

$$\Delta(u') - (\Delta u)' = -u'(\delta X)', \quad \Delta(u'') - (\Delta u)'' = -u'(\delta X)'' - 2u''(\delta X)'.$$

On the basis of these relations and once the Euler–Lagrange equation

$$\frac{\partial L_\pm}{\partial u} - \left(\frac{\partial L_+}{\partial u'}\right)' + \left(\frac{\partial L_\pm}{\partial u''}\right)'' = 0 \tag{A.6}$$

is satisfied, the variation of (A.1) reduces to

$$\begin{aligned}
\Delta A_N = &\sum_{i=1}^{N} \left[\!\!\left[\left(\frac{\partial L_\pm}{\partial u'} - \left(\frac{\partial L_\pm}{\partial u''}\right)' \right) \Delta u \right]\!\!\right]_{c_i} \\
&- \sum_{i=0}^{N-1} \left[\!\!\left[\frac{\partial L_\pm}{\partial u''} (\Delta u)' \right]\!\!\right]_{c_i} \\
&- \sum_{i=1}^{N} \left[\!\!\left[\left\{ L_+ - \left[\frac{\partial L_+}{\partial u'} - \left(\frac{\partial L_\pm}{\partial u''}\right)' \right] u' - \left(\frac{\partial L_\mp}{\partial u''}\right) u'' \right\} \delta X \right]\!\!\right]_{c_i} \\
&+ \sum_{i=0}^{N+1} \left[\!\!\left[\frac{\partial L_\pm}{\partial u''} u' (\delta X)' \right]\!\!\right]_{c_i},
\end{aligned} \tag{A.7}$$

where we have used (A.4), and $[\![A]\!]_x = A(x^+) - A(x^-)$ to denote the discontinuity at x of any quantity A. The independent variation of $(\Delta u)'$ and $(\delta X)'$ at $x = 0$ and $x = 1$ gives the "natural" boundary conditions

$$\frac{\partial L_+}{\partial u''}(0) = \frac{\partial L_+}{\partial u''}(1) = 0. \tag{A.8}$$

Conditions (A.8), which state that the "Cosserat-type" moments at the ends of the bar must vanish, prescribe a special interaction with the loading device which does not constrain the strain-gradients at the ends of the bar (zero imposed moments, the analog of a hinge).

Now, the first variation (A.7) reduces to a sum of singular terms at the points c_i and at the ends of the bar. Because we have assumed that the variations $(A.2)_1$ must be at least C^1, this implies

$$[\![\delta X]\!]_{c_i} = 0, \quad [\![(\delta X)']\!]_{c_i} = 0. \tag{A.9}$$

Regarding the smoothness of variations $(A.2)_2$, different physical assumptions can be made and we suggest two alternative models.

Model 1. (Instantaneous adjustment of the "internal variables") assumes that

$$[\![u]\!]_{c_i} = 0 \quad \text{and} \quad [\![u']\!]_{c_i} = 0, \tag{A.10}$$

which implies

$$[\![\Delta u]\!]_{c_i} = 0 \quad \text{and} \quad [\![(\Delta u)']\!]_{c_i} = 0. \tag{A.11}$$

Model 2. (No adjustment of the "internal variables") is based on a different set of conditions

$$[\![u]\!]_{c_i} = 0 \quad \text{and} \quad [\![u']\!]_{c_i} = 0, \tag{A.12}$$

which in turn implies

$$[\![\delta u]\!]_{c_i} = 0 \quad \text{and} \quad [\![(\delta u)']\!]_{c_i} = 0. \tag{A.13}$$

The physical meaning of the variations is quite different depending on whether conditions (A.10–11) or (A.12–13) are assumed. This reflects the possibility of two different phenomena occurring in phase transitions in solids.

Remark. The variations defined by (A.10–11) follow rather closely the tradition of Weierstrass (non-smooth extremals) and Gibbs (phase-equilibrium conditions). They allow for competitors that are of class C^1, but with the constraint that the competing fields have possible discontinuities of their second and higher derivatives only at the varied position (A.5) of the transition points. Thus, in Model 1, only at the points where a transition of phase occurs, i.e. of energy branch, can the competing fields have reduced smoothness; indeed, in this case a loss of smoothness in the displacement is physically possible only due to the transition itself. This is in line with the assumption made earlier that the same be true for the extremal itself.

On the contrary, the set of conditions (A.12–13) of Model 2 implies that there is no necessity for the discontinuities in the derivatives of the competitors to be located only at the varied transition points, i.e. at the points where, in the competitor, a transition of energy branch is taking place. The relevance of such variations in mechanics of crystals can be explained in terms of the interplay between "macroscopic" variables (such as strain) and "microscopic" or "internal" variables. Examples of these are the "shift" vectors used to describe the configurations of the "motif" of atoms inside a multi-lattice cell, or the parameters characterizing fine arrangements of phase variants.

While a variation in the macroscopic variables is taking place (such as a change in the strain field due to a deformation of the main lattice structure of the solid), possibly causing a movement of the discontinuities in the current configuration, the internal variables evolve following a kinetic law which is, to a large extent, independent from that of the macroscopic variables. Quite often the internal variables are observed to remain in the same "branch of

configurations" (and thus of energy) as before the variation in strain. Such phenomena are well known to occur in many circumstances in the mechanics of crystalline solids [see, for instance, the "pseudo-twinning" deformations described in Kelly and Groves (1970), or the deformations in Au–Cd alloys giving rise to shift relaxation processes, studied by Bhattacharya *et al.* (1994)], and should thus be considered in our model.

Now (A.4) can be used to obtain from (A.7) the following sets of jump and boundary conditions for extremals:

Model 1. The independent variations at c_i are Δu, $(\Delta u)'$, δX, and $(\delta X)'$, which are continuous. Hence, the following jump conditions must be satisfied by the extremals ($i = 0, \ldots, N$)

$$\left[\!\left[\left(\frac{\partial L_\pm}{\partial u'} - \left(\frac{\partial L_\pm}{\partial u''}\right)'\right)\right]\!\right]_{c_i} = 0, \tag{A.14}$$

$$\left[\!\left[\frac{\partial L_\pm}{\partial u''}\right]\!\right]_{c_i} = 0, \tag{A.15}$$

$$\left[\!\left[\frac{\partial L_\pm}{\partial u''} u'\right]\!\right]_{c_i} = 0, \tag{A.16}$$

$$\left[\!\left[L_\pm - \left(\frac{\partial L_\pm}{\partial u'} - \left(\frac{\partial L_\pm}{\partial u''}\right)'\right)u' + \left(\frac{\partial L_\pm}{\partial u''}\right)u''\right]\!\right]_{c_i} = 0. \tag{A.17}$$

Model 2. The independent variations at c_i are now δu, $(\delta u)'$, δX, and $(\delta X)'$, which again are continuous functions. In this case, the same conditions as above are obtained except for (A.17), which is replaced by

$$[\![L_\pm]\!]_{c_i} = 0. \tag{A.18}$$

Notice that in both cases, (A.16) is redundant since $[\![u']\!]_{c_i} = 0$. All the other equilibrium conditions are non-trivial, and the variational derivation clarifies their physical meaning. The two conditions (A.14) and (A.15) (obtained from the variations that change the elastic field) must be satisfied in order that the whole bar be in elastic equilibrium; they imply the balance of tractions and hypertractions (moments) at the transition points. On the other hand, conditions (A.17) or (A.18) (obtained from the variations that displace the transition points) guarantee phase-equilibrium; they are different analogs of the "Maxwell condition" of classical elasticity. We notice that the two derivations above give, in general, different equilibrium conditions. However, owing to (A.15–16), in the case of the energy (3.14), one has $[\![u'']\!]_{c_i} = 0$, and condition (A.17) becomes identical to (A.17) so that Model 1 and Model 2 are indistinguishable. However, this might not always be the case: for instance, if the interfacial energy coefficients in (3.4) are different for the two components ($\alpha_- \neq \alpha_+$), the second derivatives of the displacements are no longer continuous at the transition points and the equilibrium conditions (A.17) and (A.18) do not coincide.